

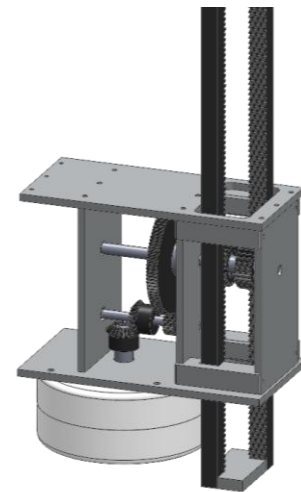
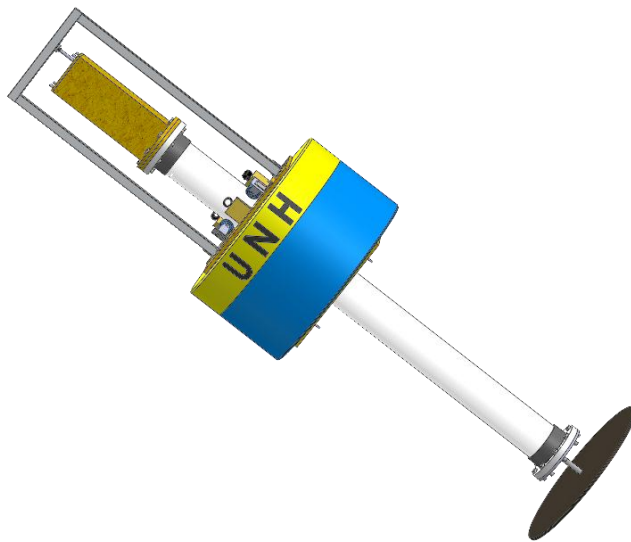


University of  
New Hampshire



# WECB: WAVE ENERGY CONVERSION BUOY

Design, Construction and Deployment of a  
wave energy conversion buoy for deployment  
at the Isles of Shoals



**Corey Sullivan, Carl Smith, Joe Henderson**

**Advisors: M. Robinson Swift, Kenneth Baldwin**

April 25, 2014

## **Acknowledgements**

This project could not have been possible without the help and guidance from numerous organizations and individuals. First and foremost we would like to extend our gratitude to our advisors Professor M. Robinson Swift and Professor Kenneth Baldwin. This project would not have been possible without the guidance from the two advisors to this project and we thank you for your clear desire to see this project succeed. Thank you to Jim Irish for lending us the follower buoy. Additional thanks should be extended to Professor Barry Fussell, Professor Michael Carter Matthew Rowell, Tobias Dewhurst, Jason Ebner and Bruce Smith for their input and aid on numerous aspects of this project. Many thanks must go to the Sea Grant Foundation and the Mechanical Engineering Department without their generous grants the budgetary needs of this project would not have been met.

# Table of Contents

<b>Acknowledgements</b> .....	<b>1</b>
<b>Table of Contents</b> .....	<b>2</b>
<b>List of Figures</b> .....	<b>4</b>
<b>List of Tables</b> .....	<b>5</b>
<b>Abstract</b> .....	<b>6</b>
Background .....	7
Objective .....	7
Concept .....	7
Motivation.....	7
<b>Preliminary Analysis</b> .....	<b>8</b>
Site Specific Wave Analysis.....	8
Linear Wave Theory .....	8
Energy Flux on Site .....	10
<b>Buoy Design</b> .....	<b>10</b>
Power Availability.....	10
Hydrostatics .....	11
Buoy Dynamics .....	14
Theoretical Spar Natural Frequency.....	16
Spar Natural Frequency Testing .....	16
Experimental Setup .....	16
Spar Testing Results .....	17
Heave Plate Considerations.....	19
Theoretical Spar with Heave Plate Natural Frequency .....	19

Spar with Heave Plate Testing and Results .....	20
Theoretical Follower Natural Frequency .....	21
Power Take-off .....	22
Gearing Theory.....	24
<b>Final Buoy Construction .....</b>	<b>25</b>
<b>Wave Tank Testing .....</b>	<b>27</b>
Tank Results .....	29
<b>Conclusions.....</b>	<b>31</b>
<b>References .....</b>	<b>32</b>
<b>Appendix .....</b>	<b>33</b>

## List of Figures

Figure 1: Schematic Describing Linear Wave Theory .....	8
Figure 2: CAD Model of Current Design .....	10
Figure 3: Schematic Illustrating Archimedes Principle .....	11
Figure 4: Center of Gravity/Buoyancy Description .....	12
Figure 5: CAD Model of Follower Buoy .....	13
Figure 6: Spar Free-Release Results .....	17
Figure 7: Spar w/ Heave Plate Free-Release Results .....	20
Figure 8: CAD Model of Power Take-Off .....	22
Figure 9: CAD Model of Dual Rack and Pinion Design .....	23
Figure 10: Model of the Gear Train in the Power Take-Off .....	24
Figure 11: Dimensioned Model of Final Design.....	25
Figure 12: CAD Model of Buoy above Water Line .....	26
Figure 13: Photograph of Completed WECB .....	27
Figure 14: Photograph of WECB in Wave Tank .....	28
Figure 15: Generator Output Voltage versus Time in Wave Tank .....	29
Figure 16: Conceptual Sketch of Hydroelectric Power Take-Off .....	35
Figure 17: OPIE Camera .....	45
Figure 18: Free-Release Test Water Line.....	45

## List of Tables

Table 1: Spar Characteristics from Free-Release Test .....	18
Table 2: Spar w/ Heave Plate Free-Release Test .....	21
Table 3: Generator Power Output and Efficiency.....	29

## **Abstract**

The Wave Energy Conversion Buoy (WECB) is a senior design project for the Undergraduate Research Projects Program for the 2013/2014 school year. The WECB team's goal is to design construct and implement a point absorber wave energy device, which will generate electrical power from ocean waves.

It is the intent of this team to demonstrate that a point-absorber wave energy device is a viable source of renewable energy to augment the current power system in place at the Shoals Marine Laboratory located on Appledore Island, Isles of Shoals, off the coast of Maine and New Hampshire. The buoy is tank tested, and then implemented for a period of time at a site located off the eastern shore of Appledore Island.

The wave energy conversion buoy that this team designed generates power by using the relative motion between two buoys, a middle buoy called the spar and a buoy that travels along the outside of the spar that is called the follower, to drive a rack and pinion gear system that turns a generator. The generator used is a three phase AC generator, which has a rated power output of 300 watts and at an ideal operating range of 400 rpm. A gear box with a 5:1 gear ratio through the gear box increases the initial rotational speed of the pinion gear due to the linear velocity of the gear rack that is attached to the follower. The power expected from the device is 300 watts for waves with an average height of 2 feet and a period of 4 seconds, assuming a device efficiency of 20 percent. These conditions are chosen because they are typical of those seen on the east side of Appledore Island for the time of year that the buoy would be deployed.

The WECB was tested in the wave tank at the Chase Ocean Engineering Laboratory to record power output from the generator. The tank was run at a 20 cm wave height with a period of 2 seconds. The available power for these wave conditions is 86.11 Watts. The voltage drop was measured across a variable power resistor and the average power output was calculated to be 12.6 Watts. Comparing the extracted power to the available produced a water-to-wire efficiency of 14.6 percent.

The following report details the findings of the WECB team in the design, construction and testing of the point absorber buoy.

## Background

### Objective

Ocean waves are phenomena that have the potential to carry a substantial amount of energy. Wave energy is the field of study focused on capturing and converting this energy into a usable form for the world's population. There are many methods, theories and devices currently in development or use today that aim to extract wave energy most efficiently from the ocean. It is the desire of this team to design a buoy that will efficiently convert the energy from these waves into usable electrical energy.

### Concept

One such device that has seen commercial use is the point absorber buoy design. The point absorber design that this team decided upon uses the relative motion between two different shaped buoys to extract energy from the waves. The general design consists of a long cylindrical center buoy called the *middle spar* and a short wide donut shaped buoy that travels along the outside of the spar called the *follower*. The relative motion experienced by the apparatus can be harnessed in numerous ways: A gearing system, a hydraulic pump, a rotational crank or a magnet and coil design are all viable options to harness the energy from the wave activity.

### Motivation

The point absorber buoy design is of particular interest to The University of New Hampshire. UNH is part of a collaborative effort in the operation and use of the Shoals Marine Laboratory (SML) on Appledore Island at the Isles of Shoals off of the coast of Maine and New Hampshire. For the most part the power needs of the lab are provided by diesel powered generators on the island. In recent years renewable sources such as solar panels and a small wind turbine have been added to aid in the powering of the lab's facilities. The point absorber buoy is an attractive option for the opportunity to add another renewable energy source to power the lab. A relatively small scale device could be placed on the seaward side of the islands to intercept the most energy possible and could be connected to the current battery bank system already in place at the island. As a laboratory, it would be beneficial to become more self-sustaining with respect to energy needs and a point absorber buoy could be a considerable asset in achieving that goal.



## Preliminary Analysis

### Site Specific Wave Analysis

Before any decisions on buoy or power take-off (PTO) components were made an analysis of the wave conditions for the proposed deployment site was conducted. The average wave conditions seen on the East coast of Appledore Island at the Isles of Shoals during the summer months were used in this analysis. The summer season off of the coast of New Hampshire provides amicable weather patterns and a relatively mild sea state to allow for observation and easy service of the buoy without fear of failure due to large winter storms and the rough seas that accompany them.

Waves with a height of 2 feet and a period of 4 seconds are the typical conditions seen at the deployment location during the summer. Linear (Airy) Wave Theory can be used to calculate parameters of interest for these wave conditions.

### *Linear Wave Theory*

Ocean waves are typically described by a set of specific parameters. These parameters are wavelength, period, wave height, and crest width. Wavelength can be described in a few ways. One of the most common is the distance between wave peaks or the distance between wave troughs. The period of a wave can be described as the time it takes for a wave to complete a cycle i.e. the time between two consecutive wave peaks. The wave height is defined as the vertical distance from peak to trough. The crest width is the distance along the wave crest perpendicular to the direction of wave propagation. These parameters can be seen in Figure 1 below.

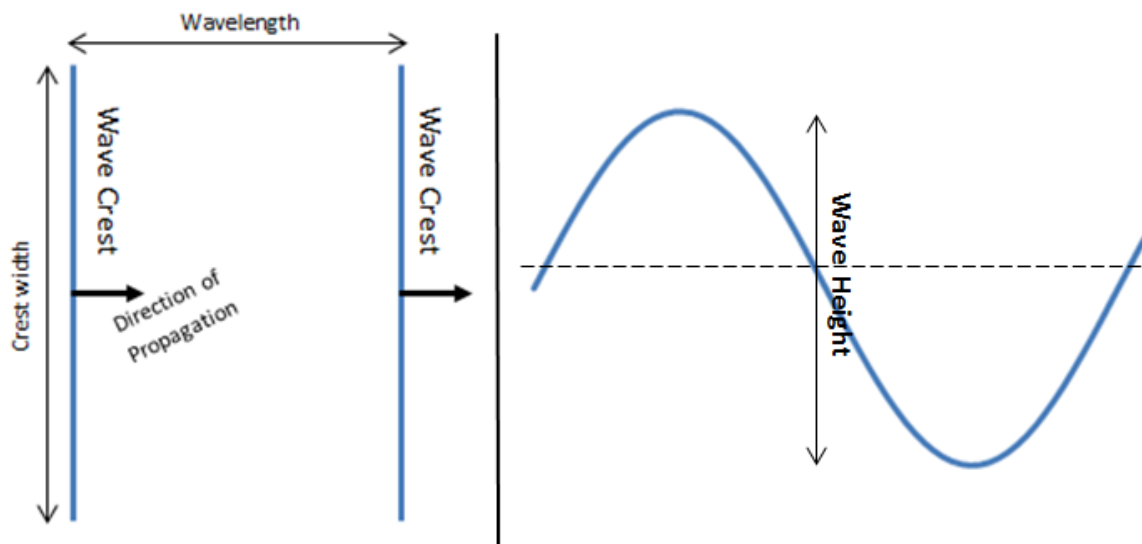


**Figure 1: Top view of ocean wave propagation with labels of relevant characteristics seen on the left. The blue lines represent the wave crests and the arrows pointing to the right indicate the direction of propagation. A side view of a propagating wave is shown to the right.**

There are a few parameters that are used extensively in linear wave theory that should be addressed. The first is the speed of a single wave, which is called the celerity of the wave. This is given by equation (1) below.

$$C = L/T \quad (1)$$

Where L is the wavelength and T is the period of the wave.

The next property that should be addressed is the wavenumber. This is a parameter based on the wavelength that is used to solve the periodicity requirements of some linear wave theory explanations that are not discussed in this report. It is given by equation (2) below.

$$k = 2\pi/L \quad (2)$$

Where L is the wavelength.

These parameters appear in many equations that dictate linear wave theory and are vital to said theory. With these parameters having been discussed other characteristics of ocean waves can be calculated. For this project the power that could be potentially intercepted by the buoy from the waves is of interest. The next few equations are parameters that allow for this calculation.

From linear wave theory one can calculate the energy and power expected from waves of certain characteristics. Linear wave theory states that the total average energy contained within a wave per unit crest width is given by equation (3) below.

$$E = \frac{1}{8}\rho g H^2 \quad (3)$$

Where  $\rho$  is the density of water,  $g$  is the gravitational constant and  $H$  is the wave height. This value  $E$  is termed the energy per unit surface area.

Another parameter called the group velocity can be calculated and is needed be able to find the power intercepted from the waves.

$$C_g = \frac{1}{2} \left( 1 + \frac{2kd}{\sinh(2kd)} \right) * C \quad (4)$$

Where  $d$  is the depth of the water  $C$  is the wave celerity given by equation (1) and  $k$  is the wave number seen in equation (2).

The multiplication of the values from equations (3) and (4) calculates the rate at which a propagating wave transmits energy, denoted as energy flux. This value is given by equation (4) below.

$$F = E * C_g \quad (5)$$

Where  $E$  is the energy per unit crest length and  $C_g$  is the speed at which energy transmits also known as the group velocity which is given by equation (4).

The energy flux calculated in equation (5) is the power transmitted by the wave per unit crest width. By multiplying this value by a width measurement the power for a specific section of the wave can be calculated. This energy flux provides a guideline from which particular pieces of the buoy can be designed.

### Energy Flux at Proposed Site

Using the equations listed above the energy flux for the conditions at the Shoals was calculated to be 1,423 Watts per unit length along the wave crest.

## Buoy Design

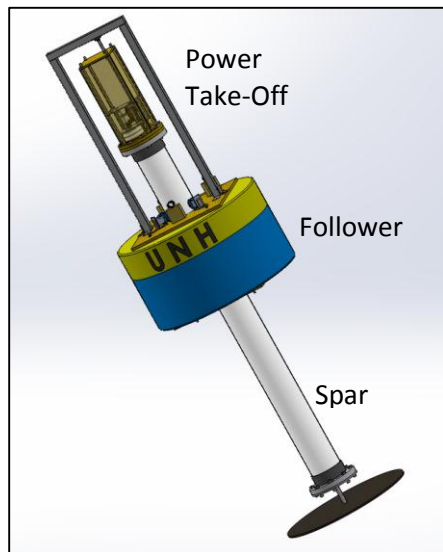


Figure 2: CAD Model of the current WECB model assembly.

The point absorber design chosen uses the relative motion between two buoys to drive a generator. Figure 2 shows a CAD model of the current WECB design. The three main components of the buoy are the middle spar, the follower, and the power take-off. The spar is intended to remain motionless in the water column, while the follower oscillates in response to the passing waves. Attached to the top of the follower is the external frame. A connecting rod feeds from the external frame into the power take-off housing, and couples with the rack mechanism. The linear motion of the connecting rod is translated into rotational motion by the rack and pinion system. As the follower heaves, the motion is transferred through this connection system, in turn spinning the gear train and generator.

The overall size of the device is selected based on the power available for the wave conditions expected at the site location. An initial analysis is performed to see how the size and mass of the spar and follower effect the hydrostatics and dynamics of the device. By selecting the size and mass necessary for the desired behavior of each buoy, the power take-off and connection system can be sized accordingly.

### Power Availability

The available power a point absorber can extract from waves of a specified height and period is quantified by the waves' energy flux multiplied by the breadth of the device, or more simply

$$P_{available} = F * b \quad (6)$$

For the WECB, the breadth,  $b$ , is represented as the diameter of the follower. In theory, designing the follower with a very large diameter would provide the device with a very large amount of available power. However, as the diameter of the follower approaches the size of the wavelength, the buoy will no longer heave uniformly with the change in the wave's surface elevation, making the device ineffective. With this in mind, along with the consideration of size limitation due to tank testing, storage, transportation, and on-site deployment, the target size for the diameter of the follower is roughly 3 to 4 feet. Coincidentally, an unused foam float previously used as a weather buoy was available in the Jere A. Chase Laboratory with a diameter of 3.5 feet. The amount of power available for a buoy of this size is 1500 watts.

Common efficiencies of point absorber energy devices of this nature are around 20%. By using this efficiency, the actual energy converted into usable electrical power is estimated to be around 300 watts for the selected buoy diameter. Based on this power expectation, the design and selection of the gear train and generator can be made and is discussed later.

### Hydrostatics

To ensure the device maintains proper stability and submerged depth in static and dynamic water conditions, ballast calculations for the spar were made using Archimedes principle so that it would not topple with a chosen draft.

Archimedes' Principle states that "the buoyancy force is equal to the weight of the weight of the fluid the object displaces" (Dean & Dalrymple) or

$$F_B = \rho_w * V_s * g \tag{7}$$

Where  $\rho_w$  is the density of the fluid  $V_s$  is the submerged volume of the object and  $g$  is the acceleration due to gravity. Figure 3 below illustrates this concept.

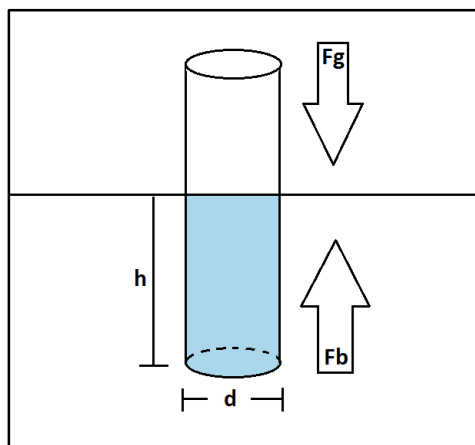


Figure 3: Schematic showing basic concept of Archimedes' principle for a spar shaped object.  $h$  is the length the object is submerged, and  $d$  is the diameter.  $F_g$  is the weight of the object and  $F_b$  is the buoyancy force acting against it.

To maintain equilibrium of the buoy the buoyancy force needs to be equal to the weight of the buoy. By equating these two terms an expression for the total mass needed to submerge the buoy with a uniform cross sectional area at a fixed depth can be written as

$$m_{total} = \rho_w * h * A_p \tag{7}$$

The ballast needed to meet the total buoy mass requirement for a particular draft can then be written as

$$m_{ballast} = m_{total} - m_{buoy} \tag{8}$$

The stability of the buoy is determined by examining the location of the center of mass in relation to the center of buoyancy. The center of buoyancy is located at half the depth of the submerged body, while the center of mass is located at the point in the object where the sum of the distributed mass sums to zero. For a stable buoy the center of mass is located lower than the center of buoyancy illustrated in Figure 4.a. The buoy becomes unstable if the center of mass rises above this center of buoyancy and will topple as illustrated in Figure 4.b.

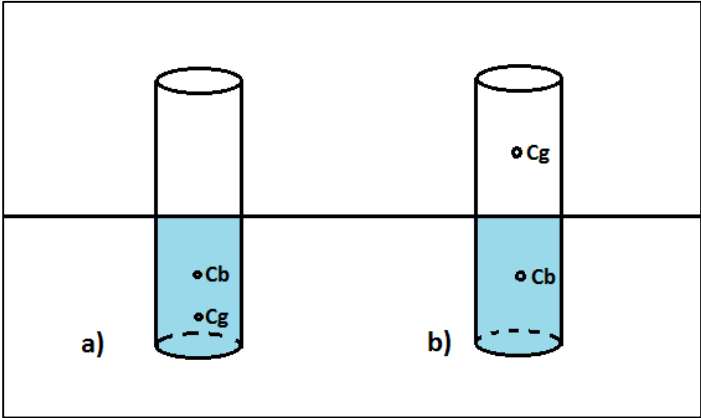
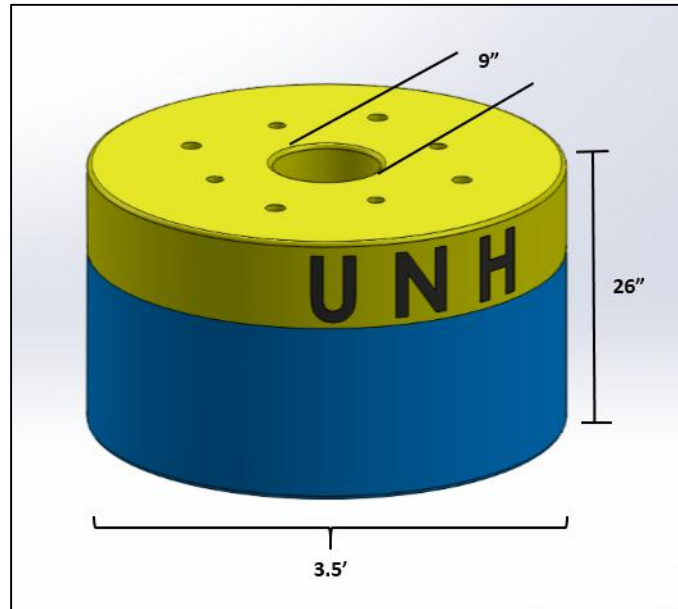


Figure 4: (a) represents a stable buoy with the center of mass lower than the center of buoyancy. (b) represents an unstable buoy with the center of mass above the center of buoyancy. The unstable buoy is not a desired design and will topple.

The dimensions of the follower that was available constrain the final sizing of the middle spar to a certain extent. Figure 5 below illustrates these dimensions.



**Figure 5: Follower buoy dimensions. Units in English customary.**

Because the spar is intended to sit inside the follower, the limiting diameter size is 9 inches. The height of the follower also limits the design of the spar. For the follower to have an upstroke, the spar must have enough freeboard above the waterline so that the follower won't hit the PTO housing.

With these considerations in mind, initial middle spar shapes were modeled in Solidworks. Using the mass properties tool to determine the location of the center of mass relative to the center of buoyancy, the final sizing with associated draft and ballast requirements were made for the middle spar. The spar size selected is 9 feet in length, 8 inches in diameter with a draft of 6 feet.

For the spar to sit in the water with a draft of 6 feet, the total mass required is roughly 140 lbs. The mass of the spar with the inclusion of the PTO and housing was roughly 70 lbs., leaving 70 lbs. required for ballast.

The follower is intended to draw roughly 5 inches of water, leaving 21 inches above the waterline giving a maximum allowable upstroke of 15 inches. To reach a draft of 5 inches, the follower requires a total mass of 240 lbs. The mass of the follower itself is 50 lbs, assuming an external frame weight of 30 lbs. the required ballast needed is 160 lbs.

## Buoy Dynamics

When exploring design options for the final product it was important to consider the natural frequencies of each buoy. As previously mentioned the point absorber design that was chosen is based on the idea that the center spar buoy remains motionless in the water column. To achieve this it should be designed with a natural period that is much longer than the period of the waves it will encounter. The higher the natural period of the spar is the less likely the spar is to react to the passing waves. The average period of the waves seen at the Isles of Shoals is 4 seconds.

Note that the natural frequency of an object is equal to  $2\pi$  divided by the natural period therefore a larger natural period corresponds to a smaller natural frequency. The motion experienced by the center spar buoy in the WECB team's assembly can be modeled as a second order system. The second order system characteristics can be described by known and variable parameters of the buoy.

More specifically a buoy's motion given an initial displacement is reminiscent of a damped harmonic oscillator. The forces on the buoy are such that these forces can be translated into components of the equation describing a second order system shown in equation (9).

$$m\ddot{x} + B\dot{x} + kx = 0 \quad (9)$$

Where  $m$  is the mass of the oscillator,  $B$  is the damping constant, and  $k$  is the spring constant.

A simplified force balance of the buoy system, neglecting drag, yields the equation shown below in (10).

$$m\ddot{x} + \rho g A_p x = 0 \quad (10)$$

Where  $m$  is the mass of the system,  $x$  is the distance into the water column,  $\rho$  is the density of the water  $g$  is the gravitational constant and  $A_p$  is the planform area of the buoy which in this case would be a circle. This term is the buoyancy force experienced by the buoy which comes from Archimedes principle. Archimedes principle states that the buoyancy force is equal to the mass of the water displaced by the submerged volume of the object.

Equating the  $x$  terms from equations (9) and (10) indicates that the "spring" force in this system is the buoyancy force on the buoy.

If the damping associated with viscous drag is considered, the full equation representing the motion of the spar buoy is given by equation (11).

$$\ddot{x} + \frac{B}{m}\dot{x} + \frac{\rho g A_p}{m}x = 0 \quad (11)$$

Where  $m$  is the mass of the system,  $x$  is the distance into the water column,  $B$  is the damping constant from viscous drag, which is unknown,  $\rho$  is the density of the water  $g$  is the gravitational constant, and  $A_p$  is the planform area of the buoy which in this case is a circle.

The standard form of a second order system is shown by equation (12).

$$\frac{1}{\omega_n^2} \ddot{x} + \frac{2\zeta}{\omega_n} \dot{x} + x = 0 \quad (12)$$

Where  $\omega_n$  is the natural frequency of the system  $x$  is the distance into the water column and  $\zeta$  is the damping ratio.

If equations 3 and 4 are put in the same form and each individual part of each one is equated, relationships can be established between the real components of the system to characteristics such as natural frequency and damping ratio. These comparisons yield equations (13) and (14).

$$\frac{\rho g A_p}{m} = \omega_n^2 \quad (13)$$

$$\frac{B}{m} = 2\zeta\omega_n \quad (14)$$

Where  $m$  is the mass of the system,  $g$  is the gravitational constant,  $B$  is the damping constant from viscous drag, which is unknown,  $\rho$  is the density of the water,  $A_p$  is the planform area of the buoy which in this case is a circle,  $\omega_n$  is the natural frequency of the system  $x$  is the distance into the water column and  $\zeta$  is the damping ratio. These relationships coupled with experimental data analysis allows for calculation of unknown parameters of the system. In the case of the spar this is the damping constant and the mass of the system.

Equation 13 shows that the natural frequency of the spar decreases with an increased mass and decreases with a larger planform area. To minimize the natural period of the natural frequency of the spar smaller diameters and heavier masses should be considered.

The full characterization of the motion of the buoy needs to consider the damping associated with viscous drag. The physical mass of the buoy is known, but the buoy is oscillating in a viscous fluid where there is “added mass” to be considered. The amount of this additional consideration is unknown so the entirety of the mass is considered an unknown in the analysis.

The first step of the analysis is to use the logarithmic decrement method on the data collected from the free drop test to find the damping ratio of each oscillation recorded. The equation for the log decrement method is given in equation (15).

$$\zeta = \frac{\frac{1}{n-1} \ln\left(\frac{x_1}{x_n}\right)}{\sqrt{4\pi^2 + \left[\frac{1}{n-1} \ln\left(\frac{x_1}{x_n}\right)\right]^2}} \quad (15)$$

Where  $n$  is the number of peaks considered  $x_1$  is the magnitude of the first peak, and  $x_n$  is the magnitude of the last peak considered. The values for  $x_1$  and  $x_n$  are taken from the plotted data.

The next step is to find the damped natural period of the system. This is completed by averaging the time between successive peaks from the recorded data. Once this period is known the damped natural period is known due to the relationship in equation (16).

$$\omega_d = 2\pi/T_d \quad (16)$$



Once equations (15) and (16) are utilized the relationship shown in (17) can be used to find the natural frequency of the system.

$$\omega_d = \omega_n \sqrt{1 - \zeta^2} \quad (17)$$

Once the natural frequency and the damping ratio are found the relations seen in equations (13) and (14) are applied to find the virtual mass of the system and the damping coefficient related to viscous damping.

### ***Theoretical Spar Natural Frequency***

The buoy dynamics theory described in the previous section was used to calculate the theoretical natural frequency and period of the spar buoy. Initial designs of the buoy called for a draft of 6 feet. The mass required to sustain this amount of draft in the water was added to the spar for this test.

The theoretical natural frequency of the spar was 2.316 radians per second. This corresponds to a theoretical natural period of 2.71 seconds. These are only preliminary theoretical values and experimental data was used to validate the findings of this analysis.

### ***Spar Natural Frequency Testing***

#### **Experimental Setup**

To characterize the real-life movement of the spar buoy, an accurate model is constructed and the free-response to an initial displacement of the buoy is tracked using the OPIE system. A description of what OPIE is and how it works can be found in Appendix A.4. OPIE output is then placed into Matlab to plot the vertical displacement of the buoy versus time for several trials to allow for analysis.

The 9 foot section of pipe, with the flange and cap attached, weighs approximately 70 pounds. To mimic what the weight will be in the final assembly 70 pounds is added to the spar by placing sections of chain in the bottom of the buoy.

To demonstrate the free-response of the buoy, it is initially displaced, and subsequently released from its equilibrium position in the water. To minimize any rotational forces placed on the buoy, a string attached to the top of the PVC pipe was used to introduce the initial upward displacement. Several trials were recorded, each with an upward initial displacement of approximately 3 inches. As a source of comparison, one trial was completed with an initial downward displacement of approximately 3 inches.

## Spar Natural Frequency Test Results

Figure 6 shows the vertical displacement of the buoy with respect to time for the sixth drop trial. The blue line indicates the displacement of the bottom dot that is tracked by OPIE, the green line indicates the displacement of the top dot, and the red line shows the average displacement for the top and bottom dots.

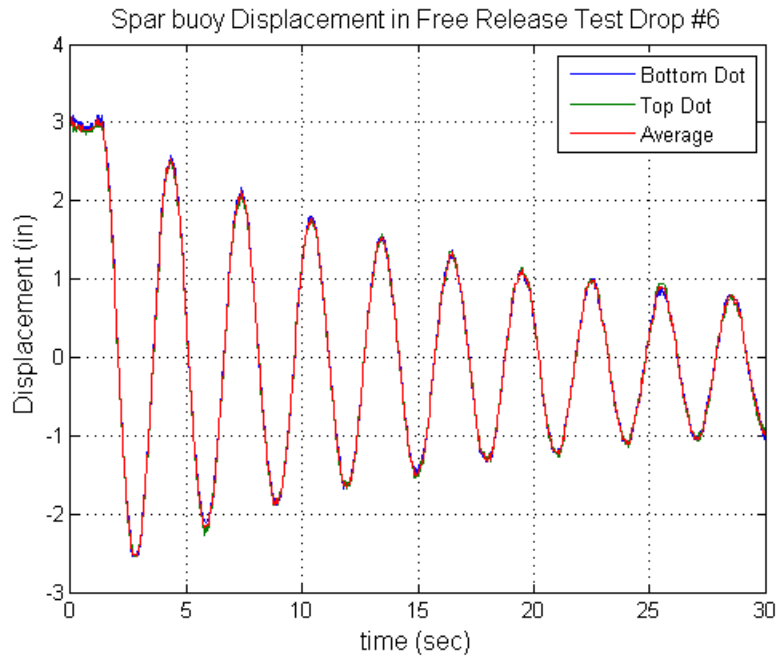


**Figure 6: Vertical displacement of the buoy with respect to time for an initial upward displacement. The blue line indicates the displacement of the bottom dot that is tracked by OPIE, the green line indicates the displacement of the top dot, and the red line shows the average displacement for the top and bottom dots.**

As expected, these waveforms are almost exactly the same, indicating there is little pitch, yaw, or roll occurring while the buoy oscillates in the water. Consequently, this drop trial provides accurate experimental data. Other drop trials which show similar accuracy can be found in Appendix A.5.

Unknown system parameters can be determined from the experimental data. Values for the virtual mass, damped natural frequency, undamped natural frequency, damping coefficient, damped natural period, and undamped natural period were calculated for all trials deemed usable, and were subsequently averaged. Table 1 shows these averaged values.

**Table 1: Values for the parameters of the spar without a heave plate, averaged over all of the trials.**

Virtual Mass :	74.0966 kg
Damped Natural Freq. :	2.016 rad/s
Undamped Nat. Freq. :	2.0721 rad/s
Damping Coefficient :	6.3026 kg/s
Damped Nat. Period :	3.033 seconds
Undamped Nat. Period :	3.0323 seconds

The actual mass of the buoy was 64 kg so there is an additional mass of 10.0966 kg due to entrainment and other fluid effects on the buoy. The damping coefficient due to viscous forces on the surface of the buoy can also be backed out of the relations used to find the virtual mass. This damping coefficient is found to be 6.3026 kg/s. The theoretical model that was initially used to predict response and behavior of the spar buoy was edited to account for the virtual mass and the viscous damping coefficient. These values will provide more accurate predictions to find the mass of the spar needed to obtain the highest natural period possible while maintaining properties the WECB team desires.

Inaccuracies in previous theoretical models can be explained by the lack of consideration of viscous damping and virtual mass. The theoretical natural frequency was 2.071 seconds which is slightly less than the experimental value of 3.03 seconds. This is an 11 percent error between the values.

The roughly 3 second natural period of the spar alone is 5 seconds shorter than the desired value. This calculation further endorsed the need to add a heave plate to the overall design of the buoy. A heave plate has an “added mass” term associated with the geometry of the plate that will effectively add mass to the system without changing where the buoy sits in the water.

### **Heave Plate Considerations**

As mentioned the addition of a heave plate adds an “added mass” to the buoy without actually changing the physical ballast of the spar. A heave plate acts as an inertial disk and resists heave motion in the water column. The added mass of a heave plate with a circular cross section is given by equation (18).

$$m_{add} = \frac{8}{3}\rho r^3 \quad (18)$$

Where  $\rho$  is the density of the fluid and  $r$  is the radius of the heave plate.

This added mass can be added to the mass in the natural frequency calculation for the spar buoy which decreases the natural frequency which in turn means the natural period increases.

### **Theoretical Spar with Heave Plate Natural Frequency**

Buoy dynamics theory was again used to calculate the theoretical natural frequency and period of the spar, this time with the heave plate installed. All other variables were intended to remain consistent with the previous free release tests.

The theoretical natural frequency of the spar with the heave plate was 0.9 radians per second. This corresponds to a theoretical natural period of 6.98 seconds. It should again be noted that these are preliminary theoretical values and experimental data was used to validate the findings of the analysis.

## Spar with Heave Plate Natural Frequency Testing

The same test method used to find the natural frequency of the spar alone was used to find the natural frequency of the spar with the heave plate attached. A plot of the heave motion of the spar and heave plate from a free drop test is shown in Figure 7 below.

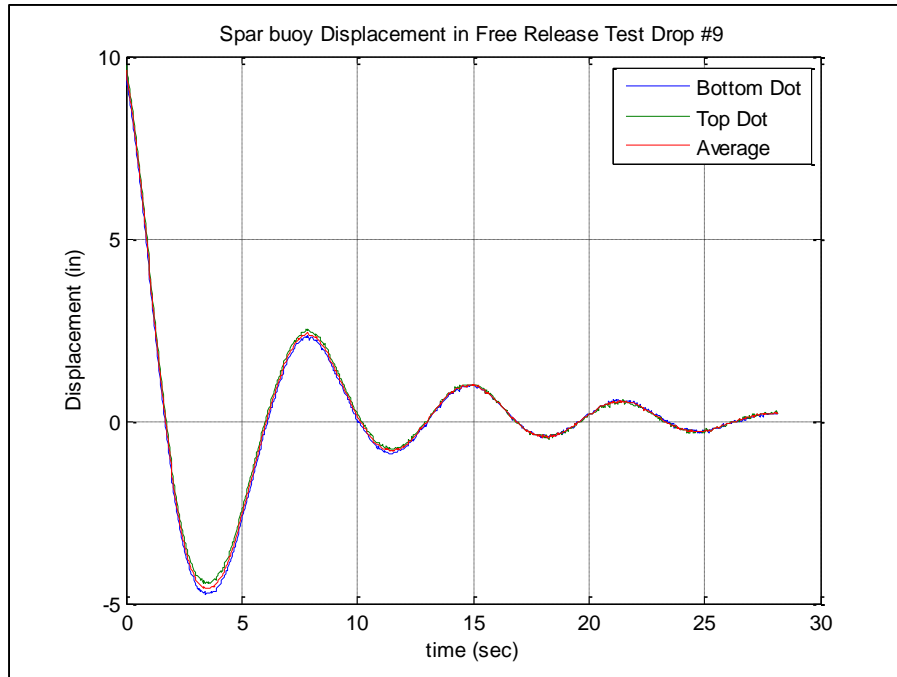


**Figure 7: Vertical displacement of the buoy with the heave plate versus time for an initial upward displacement. The blue line indicates the displacement of the bottom dot that is tracked by OPIE, the green line indicates the displacement of the top dot, and the red line shows the average displacement for the top and bottom dots.**

Initial, visual comparison of Figure 7 above to the same plot produced from the free drop test without the heave plate shows that the addition of a heave plate corresponds to a much faster damping of the oscillation of the spar. The buoy's oscillation diminishes much faster. The output averages for this set of experiments are shown in Table 2 on the following page.

**Table 2: Values for the parameters of the spar with the heave plate obtained from free release tests and analysis using the OPIE visual tracking system and software. Values shown were averaged over all of the trials.**

Virtual Mass :	358.67 kg
Damped Natural Freq. :	0.906 rad/s
Undamped Nat. Freq. :	0.948 rad/s
Damping Coefficient :	140.185 kg/s
Damped Nat. Period :	6.94 seconds
Undamped Nat. Period :	6.63 seconds

The natural period of the spar with the designed heave plate of 1 meter diameter has a natural period of more than double the natural period of the spar alone. The heave plate addition moves the natural period of the spar the closest it can get to the desired 8 seconds while maintaining logistically sound design features.

Previous theoretical models for the spar with the heave plate were quite accurate. The theoretical natural frequency was 6.98 seconds which is slightly larger than the experimental value of 6.94 seconds. There is a 0.62 percent error between the values supporting the correlation between theoretical modeling values and real results.

### **Follower Theoretical Natural Frequency Calculations**

Theoretical values of the natural frequency and period of the follower buoy were calculated using the same second order system modeling method used for the calculations of the theoretical spar frequency calculations. The theoretical natural frequency of the follower without any additional weight is 19.65 radians per second. This corresponds to a natural period of 0.32 seconds. If the weight to be added to lower the follower the desired amount and an estimate of the weight of the mounted hardware are taken into consideration these values change. With a more representative weight of the follower once it is deployed the natural frequency is 8.6 radians per second which is a natural period of 0.73 seconds. A natural period as short as this is conducive to responsiveness to many inputs which is what the follower is designed to do.

It should be noted that no OPIE analysis was done on the follower for two main reasons. The first is that the differences between the theoretical and OPIE produced natural frequencies and periods of the spar were small enough to assume that the follower's theoretical values were a good estimate of the natural frequency. The second and less conspicuous reason is that a free drop test requires a uniform displacement across the body being analyzed and the follower buoy proved to be a difficult object to displace uniformly. Without a uniform displacement the OPIE analysis does not produce data that can be adequately analyzed.

## Power Take-Off

To extract the available wave power a gear box and electrical generator are coupled. Use of a rack and pinion system allows the relative linear motion of the buoys to be converted to a rotational motion which can be applied to the generator shaft. The major factors of the power take-off design include choosing the appropriate generator and implementing a “dual rack and pinion” system.

Sizing of the generator involves determining the rated output and ideal operating speed which is driven by the expected wave conditions at the Isles of Shoals. Linear wave theory allows for the available power in each wave to be calculated. For waves with a height of 2 feet and a period of 4 seconds the available power is approximately 1500 Watts. Assuming an efficiency of 20%, similar to commercially available point-absorber wave energy devices, it can be expected that the buoy will intercept approximately 300 Watts. Therefore, a generator rated for 300 Watts at its ideal operating range is chosen. A generator with a very low ideal operating speed is chosen for this project so that a small gear ratio can be used and therefore torque is not sacrificed. This leads to the choice of a 300 Watt, 400 RPM 3-phase alternating current generator. Comparison of the ideal generator speed and the relative velocity between the follower and spar buoy leads to a 5:1 gear ratio.

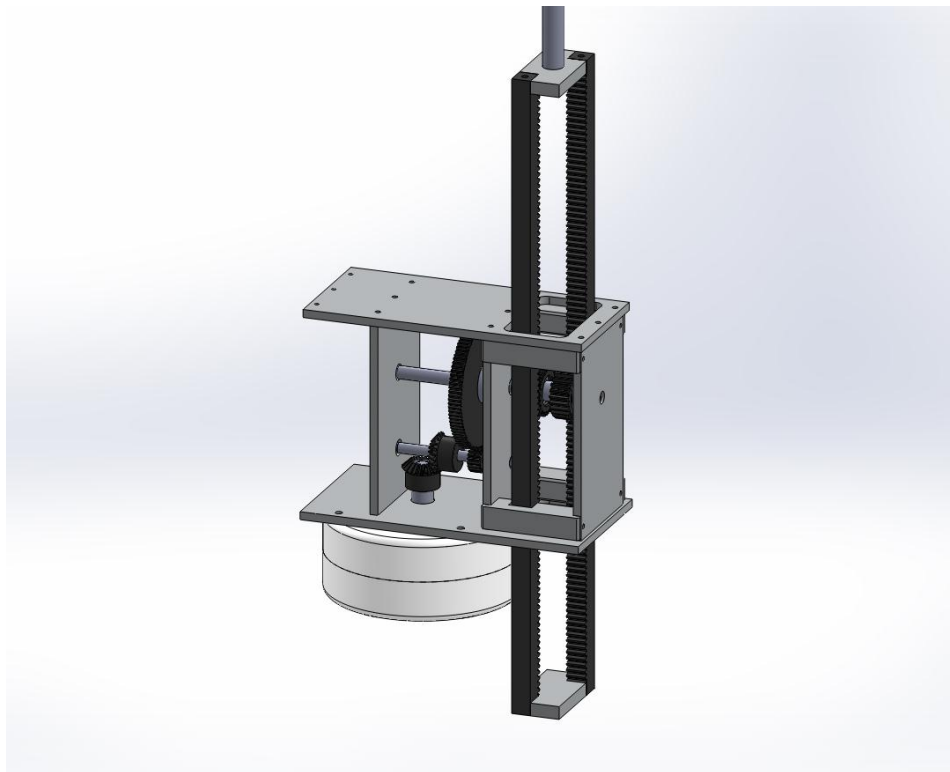
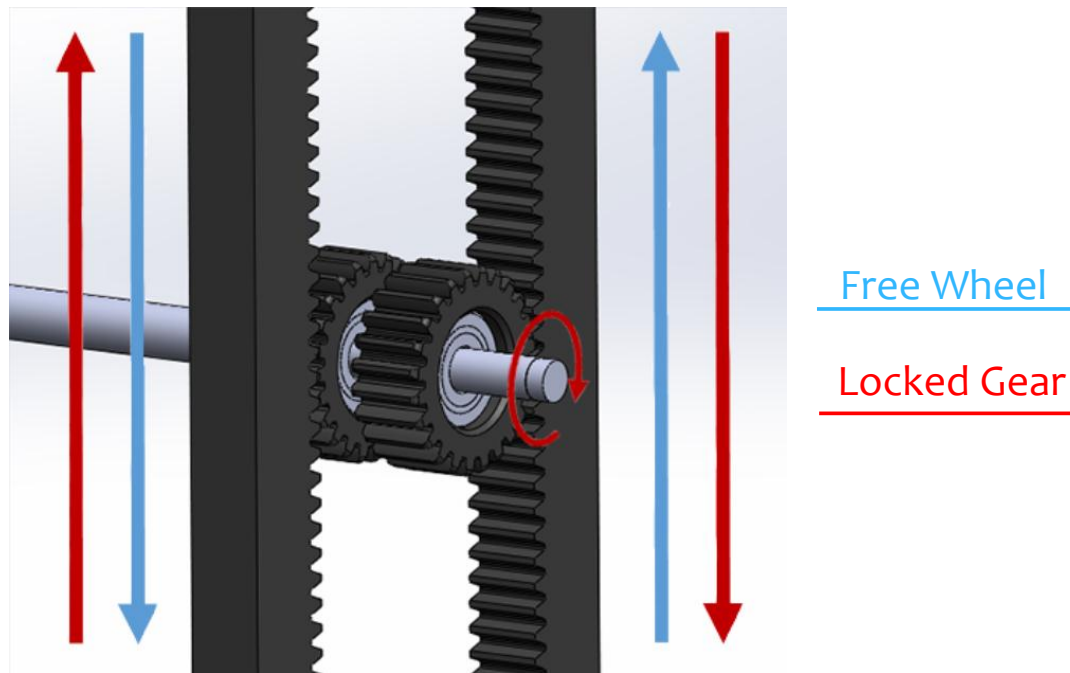


Figure 8: Solidworks CAD model of the Power Take off Assembly that is used in the Wave Energy Conversion Buoy.

Due to the oscillatory nature of waves the follower buoy changes direction every time it reaches the top or bottom of a wave. If just one rack and one pinion were used the generator shaft would change directions with each stroke as well, leading to huge inefficiencies. To address this problem a “dual rack and pinion” system is used, incorporating two racks and two pinions. Each pinion gear has a one-way clutch bearing press-it into the center allowing them to freewheel in one direction and drive in the other. On the up stroke, one bearing will drive the shaft and the other will freewheel. On the down stroke, the bearings switch roles ensuring that the shaft always spins in the same direction.



**Figure 9: CAD representation of the Dual Rack and Pinion System of the WECB. Red Arrows indicate a locked gearing driving the shaft. Blue arrows indicate a gear that is freewheeling.**

To show that the buoy is generating electricity, a lighting array comprised of 120 LEDs is connected to the generator. Since the output of the generator is 3-phase alternating current, the signal must first be converted to direct current to power the lighting array. This is achieved with an off-the-shelf bridge rectifier circuit. The rectifier accepts each of the three phases and outputs a single direct current through a positive and negative lead.



## Gearing Theory

Design of the gear box begins by assuming the spar buoy remains completely motionless in the water column and then determining the speed of the follower buoy with respect to the spar buoy, given by,

$$v = \frac{2a}{T} \quad (19)$$

Where 'a' is the wave amplitude and T is the wave period. This is also the velocity of the rack with respect to the pinion gears since the rack moves directly with the follower buoy and the pinions move with the spar. Since the chosen generator has an ideal operating angular velocity the gear ratio can be determined by,

$$\text{Gear Ratio} = \frac{\omega_{generator}}{\omega_{pinion}} \quad (20)$$

Where  $\omega_{generator}$  is the ideal operating angular velocity of the generator. The angular velocity of the pinions, dictated by the wave conditions, is calculated by,

$$\omega_{pinion} = \frac{v}{r} \quad (21)$$

Where r is the radius of the pinion and v is the velocity of the rack with respect to the pinion, presented above. This equation can be applied in general to size each gear in the gearbox until the appropriate gear ratio is reached. This is done by equating the velocity at the contact point of two meshing gears, yielding,

$$\omega_1 r_1 = \omega_2 r_2 \quad (22)$$

Where the subscripts "1" and "2" refer to the two meshing gears. It should be noted that to reduce inefficiencies the number of gears should be kept at a minimum.

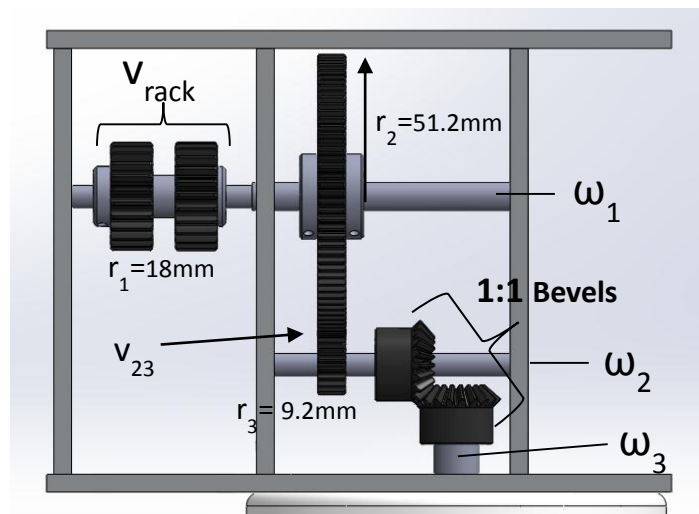


Figure 10: CAD model front view of the gear train in the power take off. Radii and rotational velocities are generically labeled.

## Final Buoy Construction

With all driving factors considered the final design is now decided upon. The major buoy dimensions are shown in Figure 11. The dimensions of both buoys, the heave plate, the power take-off, and the external frame are included.

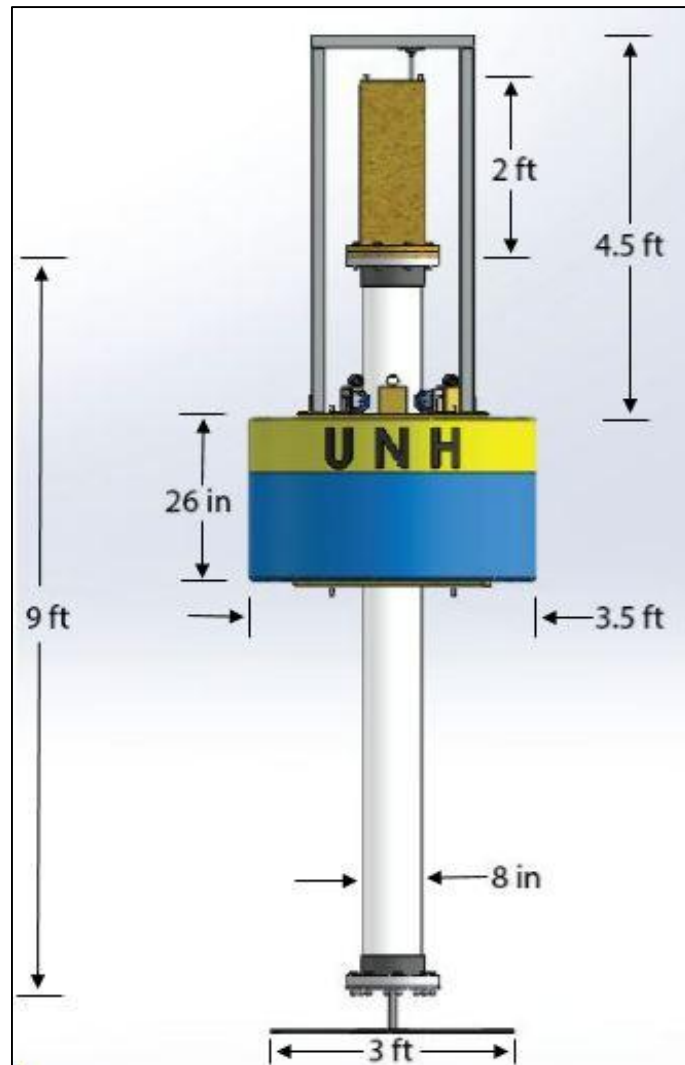


Figure 11: Overall dimensions of both buoys, the heave plate, the power take-off, and the external frame.

The spar and follower buoys must be coupled so that the relative motion between them can be used. This is achieved using the external frame which is attached to the follow buoy. The connecting rod, which is attached to the external frame via a flex coupling, enters the power take-off housing through a linear bearing and connects to the racks on the power take-off. The flex coupling helps compensate for misalignment between the connecting rod and linear bearing. The motion between the buoys is guided using castor wheels of which there are three on both the top and bottom of the follower buoy. Rubber bumpers are in place on both the top and bottom of the follower as well. These bumpers contact

stopper plates around the spar buoy in the case of larger waves than designed for. Figure 12 shows a close-up of the top half of the buoy, including the power take-off and its housing, the external frame, the connecting rod, the guide wheels, and the rubber bumpers. Not shown are the flex coupling and stop plates.

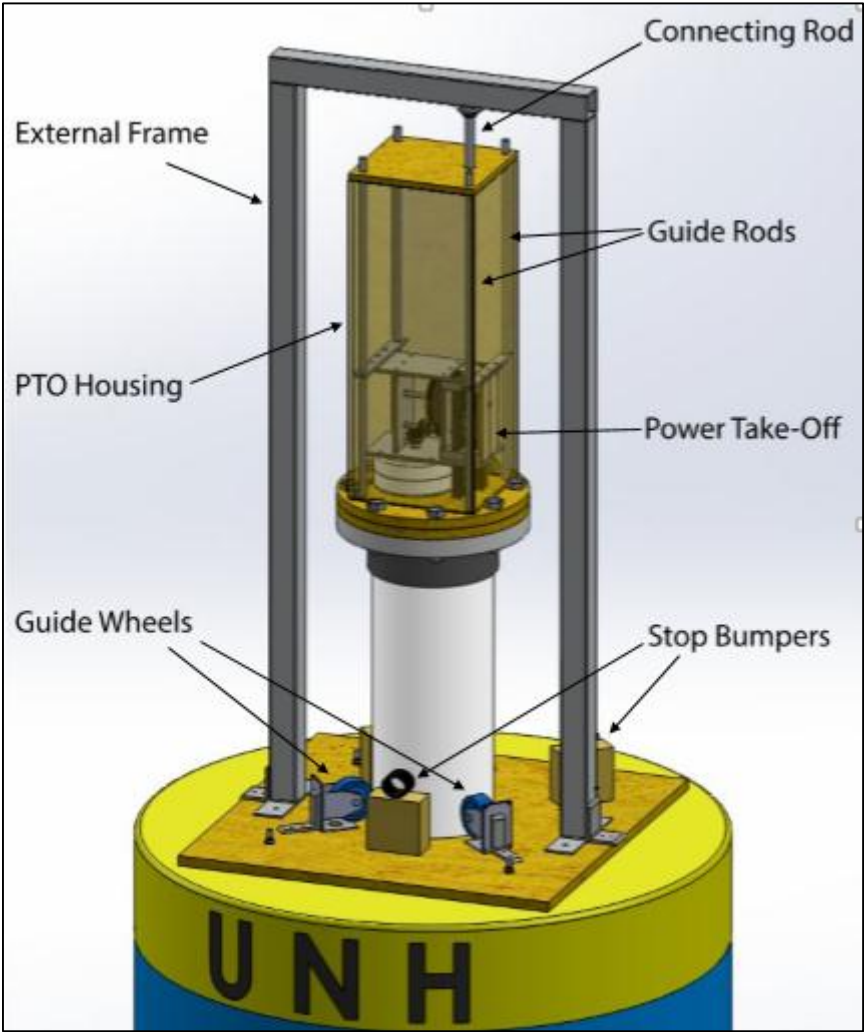
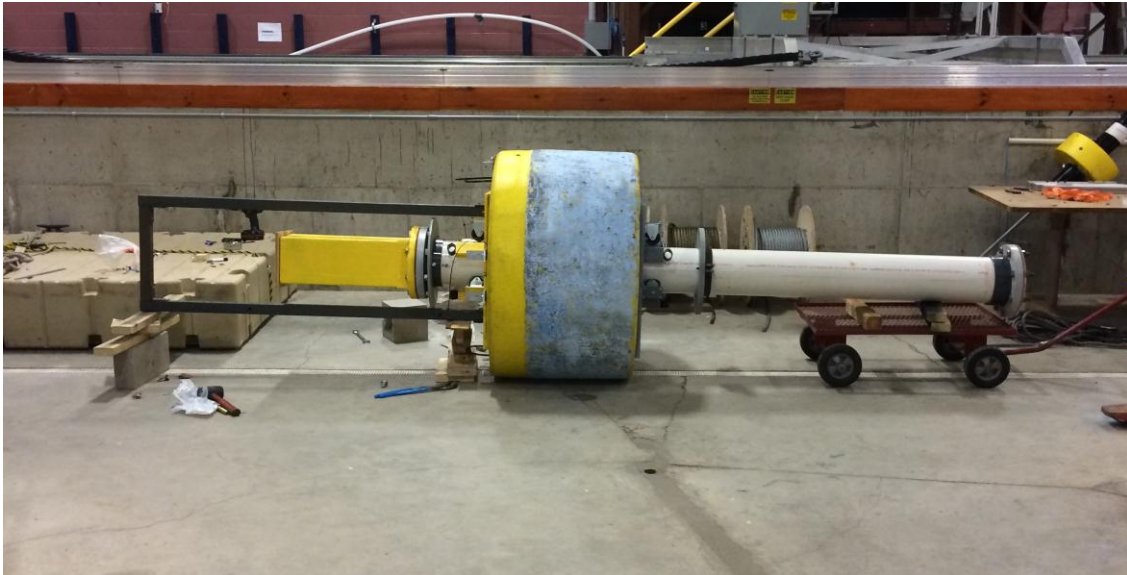


Figure 12: Main buoy components including external frame, PTO, PTO housing, guide wheels, stop bumpers, guide rods, and connecting rod.

Figure 13 below shows the WECB in its final stages of construction in the Chase Ocean Engineering Laboratory.



**Figure 13: Photograph of the Completed Wave Energy Conversion Buoy after construction.**

## **Wave Tank Testing**

After the construction of the buoy was completed second semester, the wave tank in the Jere A. Chase Ocean Engineering Laboratory was utilized to test the buoy in actual wave conditions. The wave tank provides a controlled environment to observe the buoy's capabilities. Testing in the tanks allows control of the wave height and period giving the ability to compare experimental results to theoretical values from wave theory based on the known characteristics.

The WECB is a full scale buoy and the most indicative tests for this device would be with the wave height and period closest to the wave conditions the buoy is designed for. Waves with a height of 20 centimeters and a period of 2 seconds were used as they are the closet representation of real ocean waves that could reasonably be attained in the tank. Anything beyond a 2 second period or a height larger than 20 centimeters does not produce a consistent waveform resulting in data that would be more difficult to analyze.



**Figure 14: Photograph of the Wave Energy Conversion Buoy in the wave tank at the Jere A. Chase Ocean Engineering Laboratory.**

To measure the power output from the buoy the leads from the generator were connected to a variable power resistor and the voltage drop was measured across it. Using Ohm's and Joule's laws the power output can be found with the voltage drop and known resistance from equation \_ below.

$$P = V^2/R \quad (23)$$

Where V is the voltage drop measured in volts and R is the resistance measured in ohms.

The output voltage was measured with a WinDaq digital oscilloscope and analyzed in Matlab. A small section of a voltage vs. time plot is shown below in Figure 15 below.

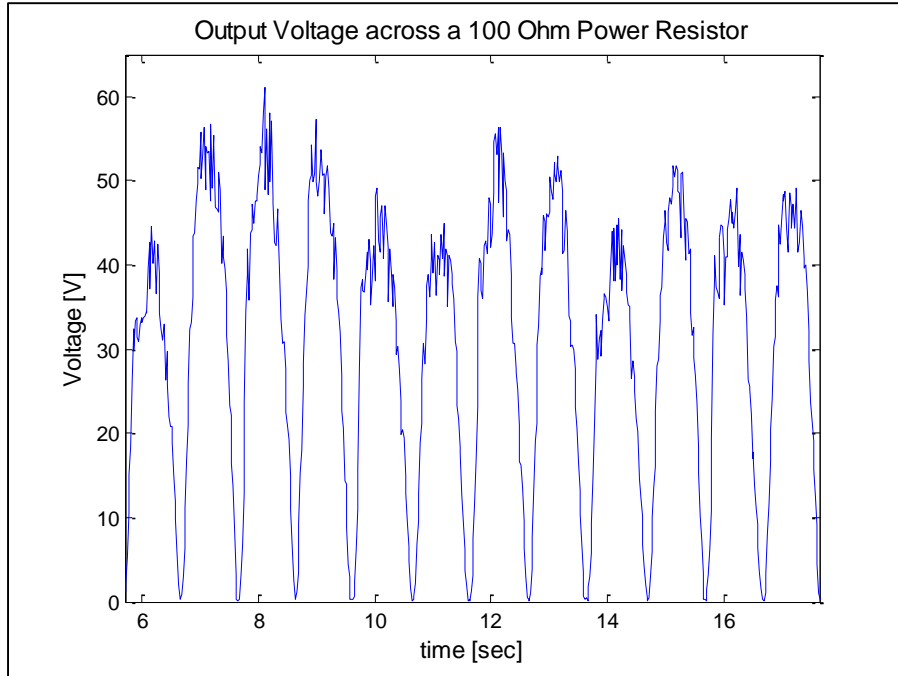


**Figure 15: Voltage vs. time plot from the WinDaq Oscilloscope. The voltage measured is the voltage drop across a variable power resistor at the 100 ohm setting. Each peak represents the up or down stroke of the rack.**

From Figure 15 it can be seen that the output from the buoy is not a continuous signal due to the oscillatory motion produced by the waves. To obtain the most representative value for the output as a whole the root mean square was taken of the data. The root mean square is a statistical measure of the magnitude of a varying quantity; the equation is given below in Equation 24. For a periodic function it gives the most indicative value for the overall signal. The 'V' value used in equation 23 is the RMS value of the voltage signal.

$$f_{RMS} = \sqrt{\frac{1}{T_2 - T_1} \int_{T_1}^{T_2} [f(t)]^2 dt} \quad (24)$$

Where  $f(t)$  is the value of the function with relation to time, and  $T_1$  and  $T_2$  are the limits of time for the portion of the output that is of interest.

The resistance that was connected to the circuit was varied to observe how the generator would react to differing potential loading scenarios. Initial investigations indicated that the lower the resistance was the harder it is to spin the generator. The first resistance tested was 300 ohms and the resistance was decreased by 50 for each subsequent test. At a resistance of 50 ohms the generator was nearly unable to move so that was the final resistance tested.

To calculate the efficiency of the buoy the power output during the test was compared to the power contained within the waves that was intercepted by the buoy. Equation (25) illustrates this equation.

$$\eta = P_{extracted} / P_{available} \quad (25)$$

For the follower buoy size in 20 centimeter waves at 2 seconds the available power from the waves is 86 Watts. A table of the power outputs for various resistive loadings and the corresponding efficiencies is shown below in Table (3).

**Table 3: Table of output voltages and efficiencies for waves produced in the Wave Tank with a 20 centimeter height and a period of 2 seconds. Resistance load on the circuit was varied to observe behavior of the system based on the resistive loads that could potentially be seen by the generator.**

<b>Power Produced from 20 cm. 2 Second Waves</b>		
<b>Resistance [<math>\Omega</math>]</b>	<b>Power Extracted [Watts]</b>	<b>Efficiency [%]</b>
50	8.2	9.5
100	12.5	14.6
150	11.1	12.9
200	12	13.9
250	11.2	13
300	8.7	10.1

The peak efficiency seen during this test was 14.6 percent with a resistive load of 100 ohms.

## Conclusions

The point absorber wave energy device under study uses the relative motion between two buoys, the inner spar buoy and the outer follower buoy, to drive an electrical generator. The wave conditions at the desired site of deployment are used to drive the design of the buoys and the power take-off system.

For this type of wave energy buoy to function, the spar buoy must remain motionless in the water column while the follower buoy moves up and down with passing waves. To achieve this it is required that the spar buoy have a natural period much larger than the period of the passing waves. Calculations showed that the spar buoy should have an 8 inch diameter and a weight of 140 pounds. A free-release test was completed on the buoy with and without a heave plate yielding natural frequencies of 3.033 seconds and 6.94 seconds, respectively. This validates the need for a heave plate.

While the spar buoy remains motionless in the water, the follower buoy must heave with the passing waves for the device to be effective. A theoretical analysis of the buoy natural period was completed. It was determined that the theoretical follower buoy natural period is 0.73 seconds. This period is much less than the wave period, as desired.

To determine the effectiveness of the system as a whole the buoy was tested in the wave tank. Wave conditions were set as close as possible to the wave conditions expected at the Isle of Shoals. A wave height of 20 cm and a period of 2 seconds were chosen. The load seen by the generator was varied during testing and the best loading condition was seen to be approximately 100 ohms. Under this loading and these wave conditions the buoy generated approximately 12.5 Watts, yielding a water-to-wire efficiency of approximately 14.6%.

Several improvements should be considered for future designs to improve the efficiency of this device. Although the dual rack and pinion system combated a major portion of inefficiency, the generator still shown to come to a stop at the top and bottom of the stroke. A flywheel would be a significant contribution to avoid overcoming start-up torque after each stroke, ensuring a greater and steadier power output. The rectifier circuit also proved to provide a considerable amount of inefficiency. Future work should aim to either put to use the raw 3-phase AC signal or purchase a higher quality circuit.



## References

Allard, Michael, Colin Fischer, Tania Grindrod, Jessica Murray, and Kyle Russ. *Wave Energy*.

Tech. Durham: U of New Hampshire, 2008. Print.

Caron, Shaun, Paul Madea, and David Kurtz. *WESML - Wave Energy at the Shoals Marine Lab*.

Tech. Durham: U of New Hampshire, 2013. Print.

Pritchard, Philip J., and John C. Leylegian. *Fox and McDonald's Introduction to Fluid Mechanics*.

8th Edition ed. Hoboken: John Wiley & Sons, 2011. Print.

Wright, James. *Development and Validation of a Robust Model to Predict the Response of Wave*

*Energy Conversion Devices*. Thesis. University of New Hampshire, 2010. Ann Arbor:

ProQuest, 2010. Print.

Dean, Robert G., and Robert A. Dalrymple. *Water Wave Mechanics for Engineers and Scientists*.

Englewood Cliffs, NJ: Prentice-Hall, 1984. Print.

Berteaux, Henri O. *Buoy Engineering*. New York: John Wiley & Sons, 1976. Print.

"Ocean Wave Energy." *BOEM Homepage*. U.S. DOE, 2013. Web. 12 Oct. 2013

Rvoorhis. "Energy and the Environment-A Coastal Perspective." - *Point Absorbers: The*

*Technology and Innovations*. University of North Carolina, 25 July 2012. Web. 17 Nov.

2013.

## Appendix

A.1 Future Work .....	34
A.2 Alternate Design Considerations .....	35
A.3 Conceptual Design Sketches.....	37
A.4 OPIE: Optical Positioning Instrumentation and Evaluation .....	45
A.5 Additional Free Release Test Plots.....	46
A.6 Bill of Materials and Budget as of 4/25/2014 .....	46

## **A.1 Future Work**

The eventual goal of this project is to use the WECB to provide consistent power to the Isle of Shoals for extended periods of time. To achieve this there is a considerable amount of work to be completed in the future by both the current team and future teams.

The current team plans to deploy the WECB in the ocean for a short period of time. Data acquisition will not be performed during this deployment due to time constraints. It will be useful, though, to watch how the buoy responds to real ocean conditions.

For future teams there is a considerable amount of work to be done. Refinement of the power take-off design is essential. A major improvement suggestion is to add a flywheel to the shaft of the generator. This will prevent the generator from stopping at the top and bottom of the stroke. Other components of the buoy, especially those exposed to the ocean environment, should be built more robust. With both of these improvements in place, future teams should setup an on-board data acquisition system and deploy the buoy for an extended period of time.

## A.2 Alternate Design Considerations

### Additional Power Generation Considerations

There are numerous ways to harness the energy that the device is intercepting from the ocean conditions. The three options that are most prevalent in the field at this point in time are that of a hydraulic system that pumps a working fluid past an impeller that spins a generator. Another option uses the principle of converting vertical motion to rotational motion to spin a generator via a crank system.

Before the dual rack and pinion design was finalized, an initial hydroelectric design was considered as a possible means of power generation. Figure 16 below illustrates the basic concept.

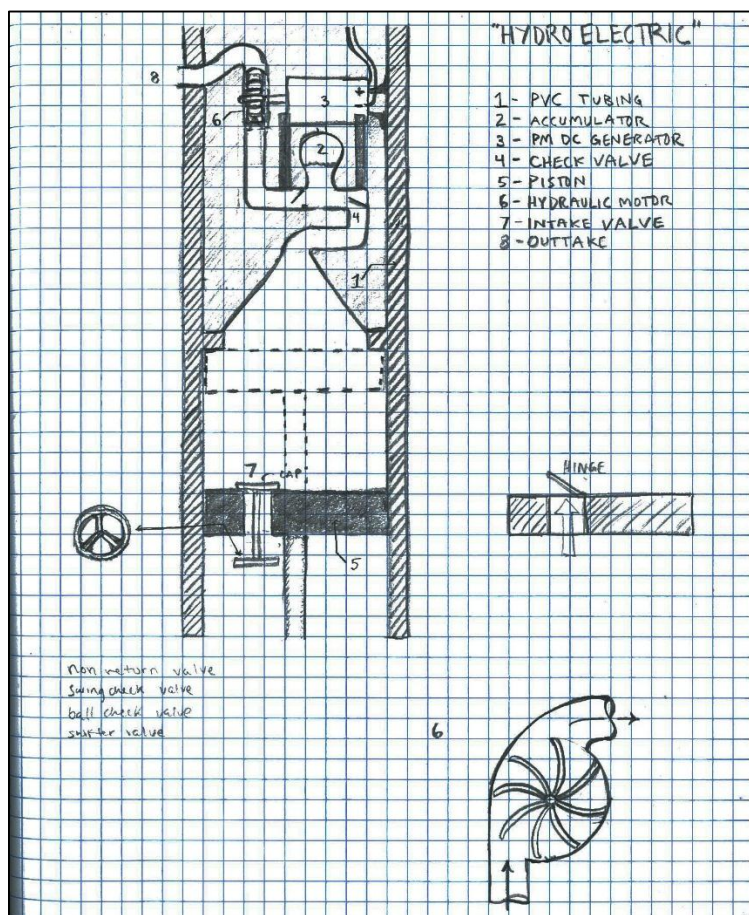


Figure 16: Hydroelectric Conceptual Sketch. Represents hydroelectric power generating device inside of middle spar.

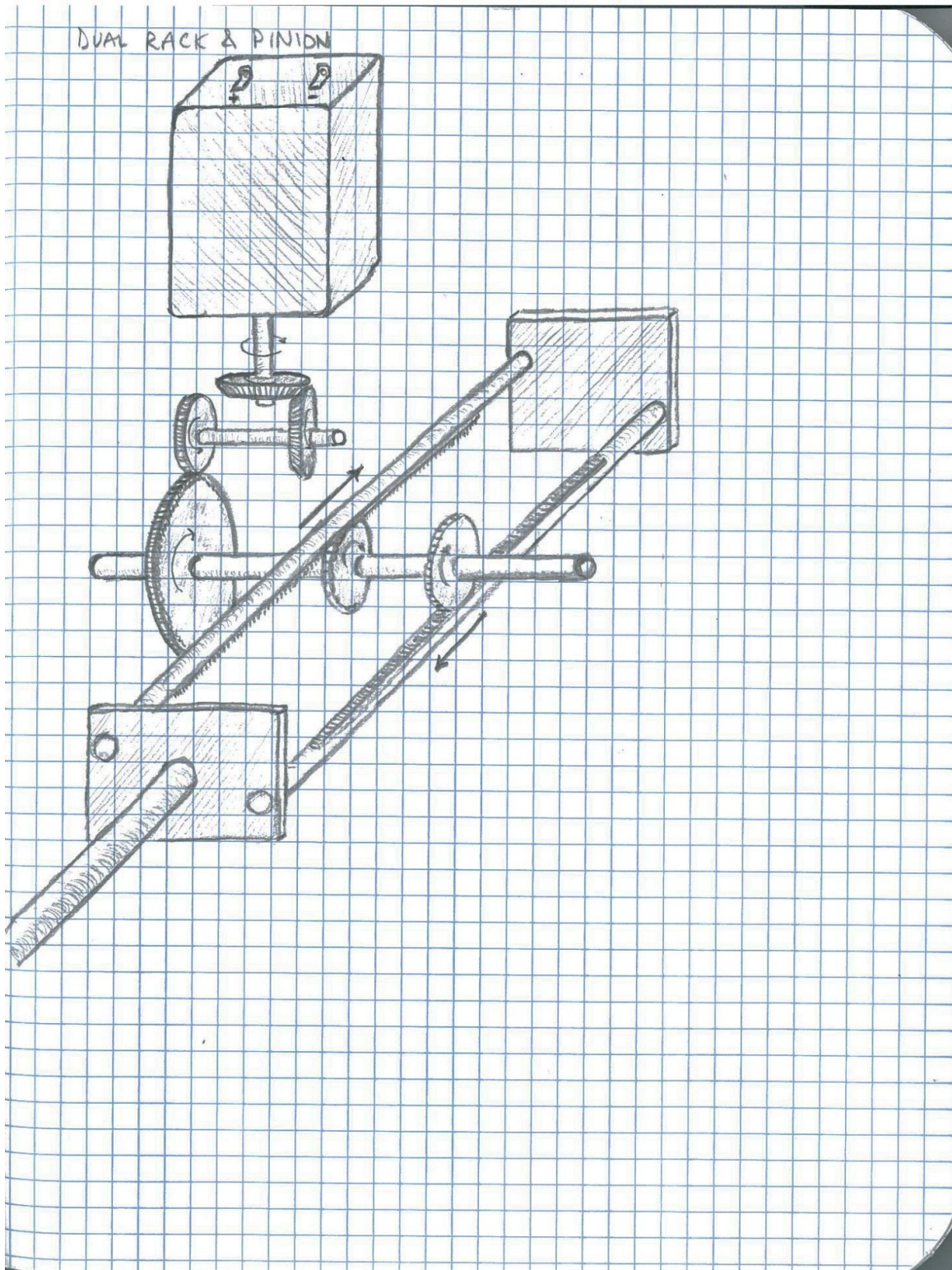
By using the ocean water as the working fluid and thrusting it through an open cycle piping system, a hydraulic motor could be used to spin the generator. This design would still use the middle spar, however its bottom would be open to the ocean water. The water is first brought into the spar through the intake valve, and is pumped through the system by the piston, which uses the middle spar inner walls as the cylinder. Using check valves and an accumulator, the water is pumped up through the hydraulic motor turbine to the exit outtake. The concept was eventually discarded, because the design would only generate power on the upstroke.

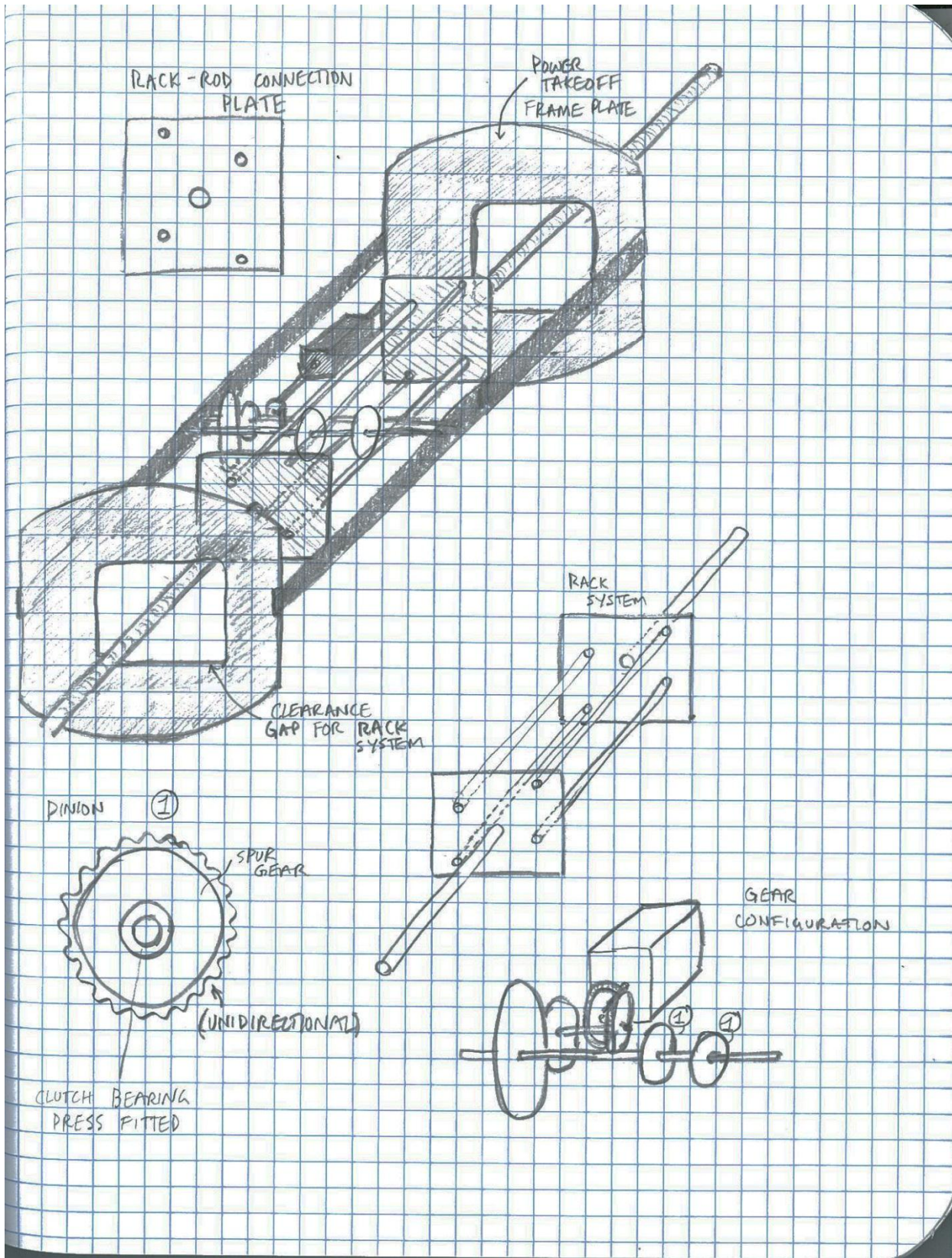
### **Location of PTO**

It was initially considered to house the power take-off inside the spar rather than on top. Housing the power take-off inside the spar would bring down the center of the gravity, adding stability to the spar buoy. This was decided against for several reasons, however. The 8 inch diameter of the pipe proved to be a difficult space constraint to work around. Using a custom sized box fixed this issue. The box also allowed for ease of maintenance since the power take-off could be taken out easily. Finally, placing the housing on top of the spar allowed the power take-off to sit well above the water line, protecting it from water in the case that the spar buoy leaks.

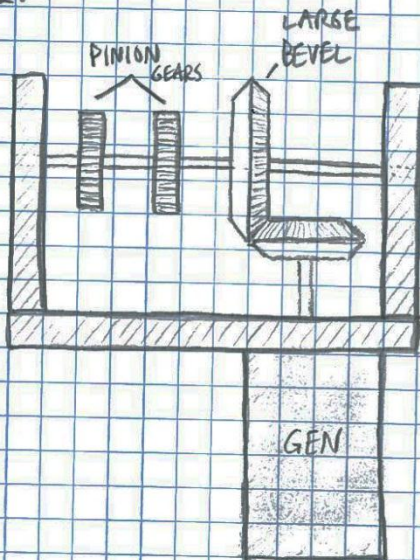
### A.3 Conceptual Design Sketches

Drawn by Carl Smith





### OPTION 1:



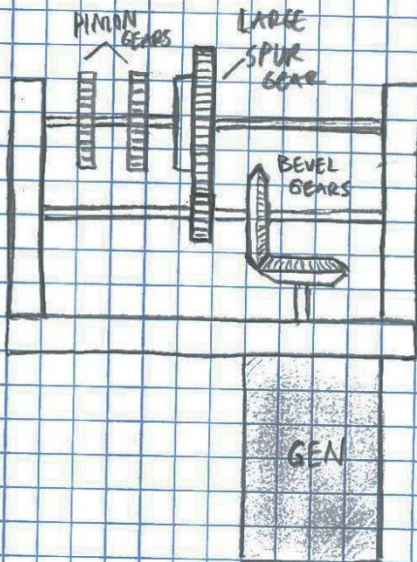
#### PROS:

- COST EFFECTIVE
- SIMPLE
- LESS MOVING PARTS
- LESS CONTACT POINTS  
(POTENTIAL DISSIPATIVE FORCES)

#### CONS:

- GEAR RATIO (GEAR UP  
LARGE BEVEL TO ACCOUNT  
FOR LOSS OF MULTIPLIER  
LINKAGE IN OPTION 2)

### OPTION 2:



#### PROS:

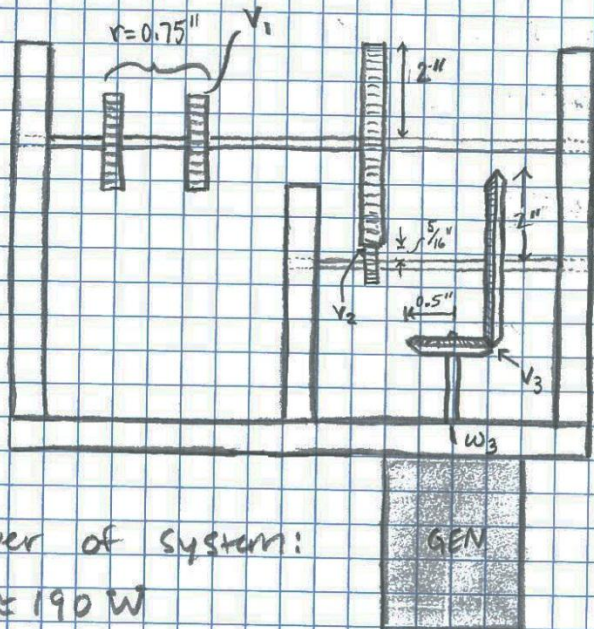
- MORE CONTROL OF  
GEAR RATIO (TO REACH  
OPTIMAL RPM)

#### CONS:

- COST (MORE PARTS)
- MORE CONNECTION POINTS
- MORE COMPLEX
- SPACE CONSTRAINTS
- MORE CONTACT POINTS



# GEAR CONFIGURATION



$$V_1 = .5 \text{ ft/s}$$

$$V_2 = 1.33 \text{ ft/s}$$

$$V_3 = 8.533 \text{ ft/s}$$

$$\omega_1 = 8 \text{ rad/s} = 1.27 \frac{\text{cycles}}{\text{sec}} = 76.2 \text{ rpm}$$

$$\omega_2 = 51.2 \text{ rad/s} = 8.198 \frac{\text{cycles}}{\text{sec}} = 488.9 \text{ rpm}$$

$$\omega_3 = 204.79 \text{ rad/s} = 32.59 \frac{\text{cycles}}{\text{sec}} = 1955.6 \text{ rpm}$$

GEAR RATIO  $\rightarrow 25.56 : 1$

Power of system:

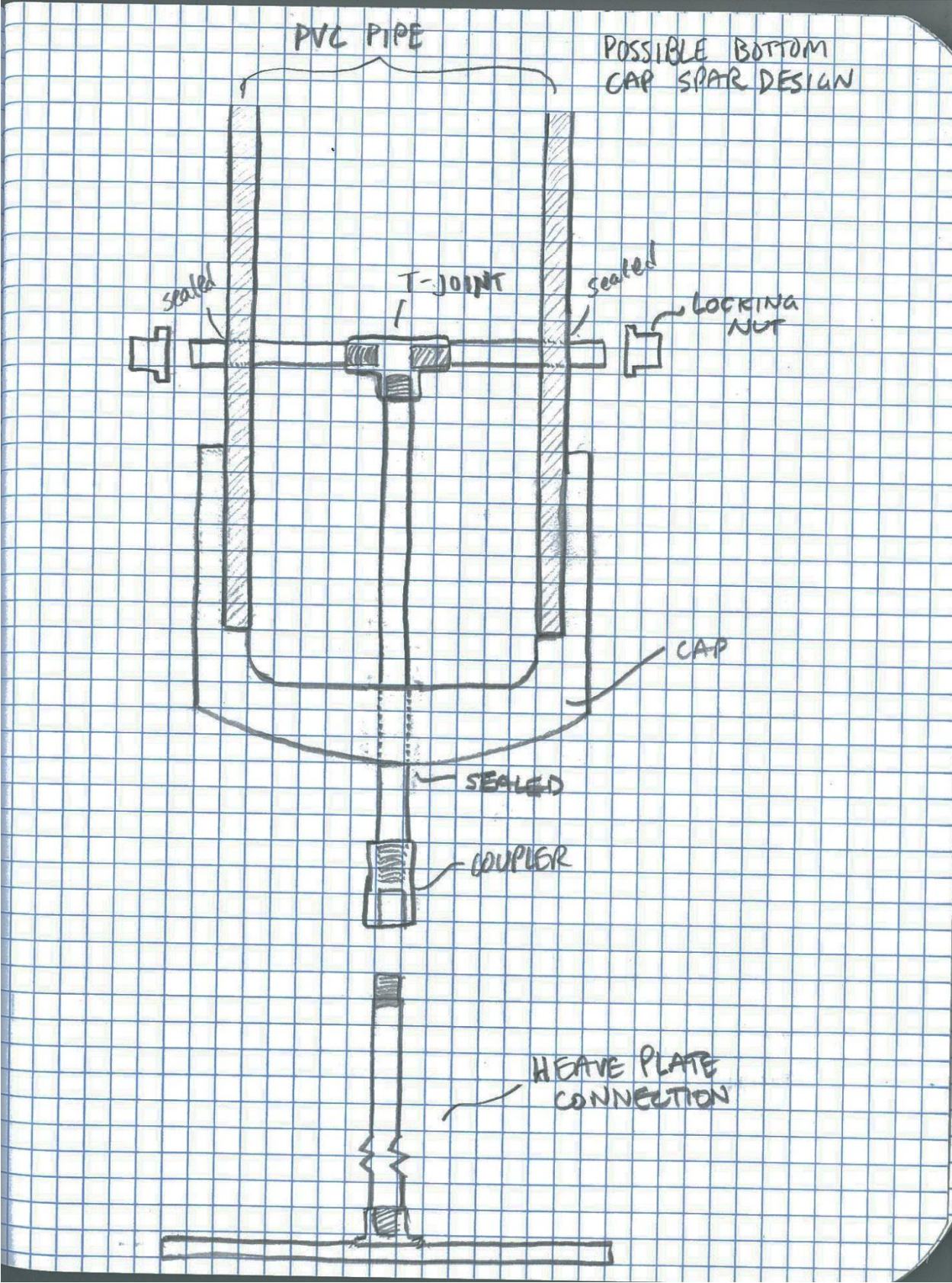
$$\approx 190 \text{ W}$$

low  $\approx 100 \text{ W}$ ?

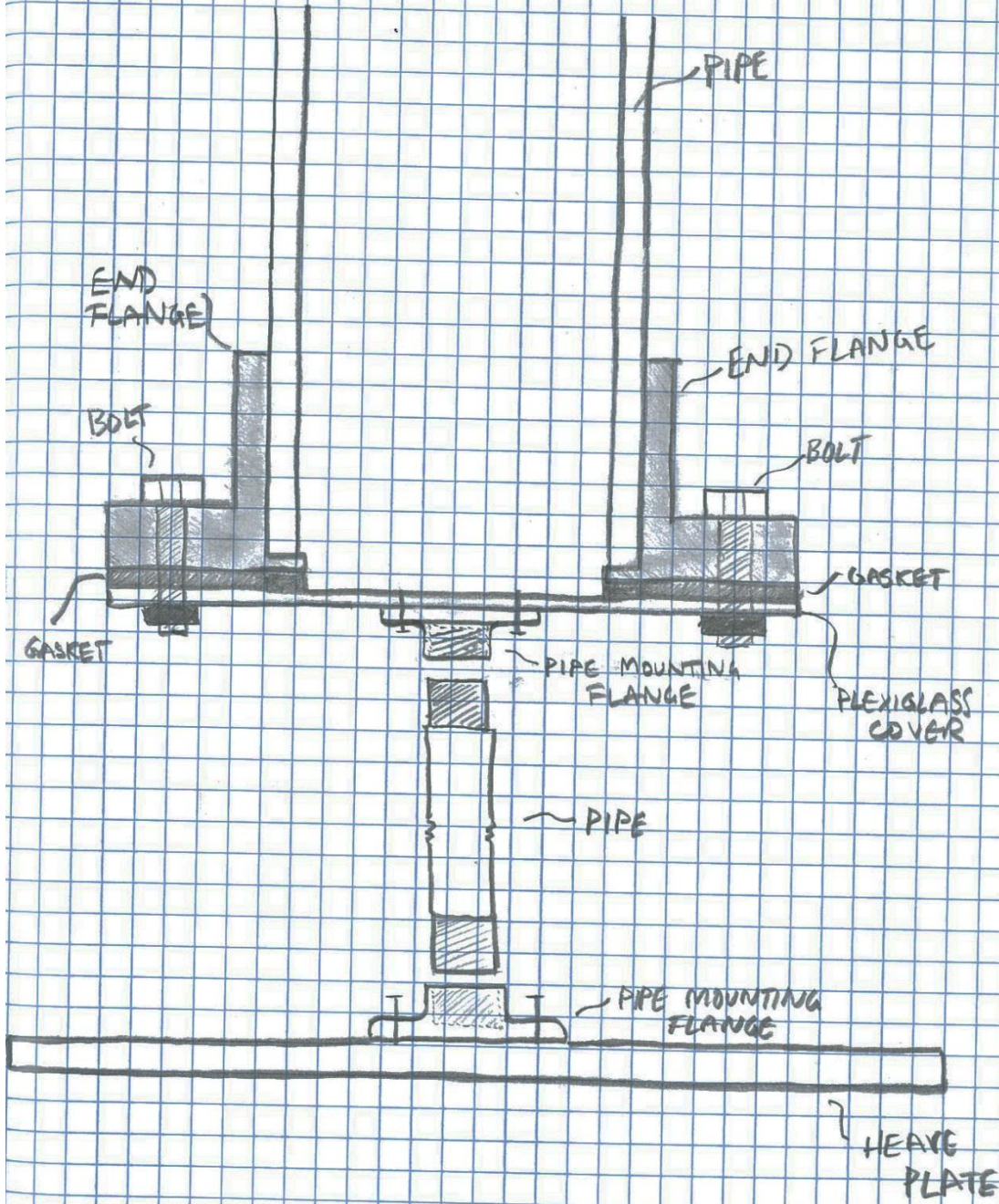
$$P = T\omega$$

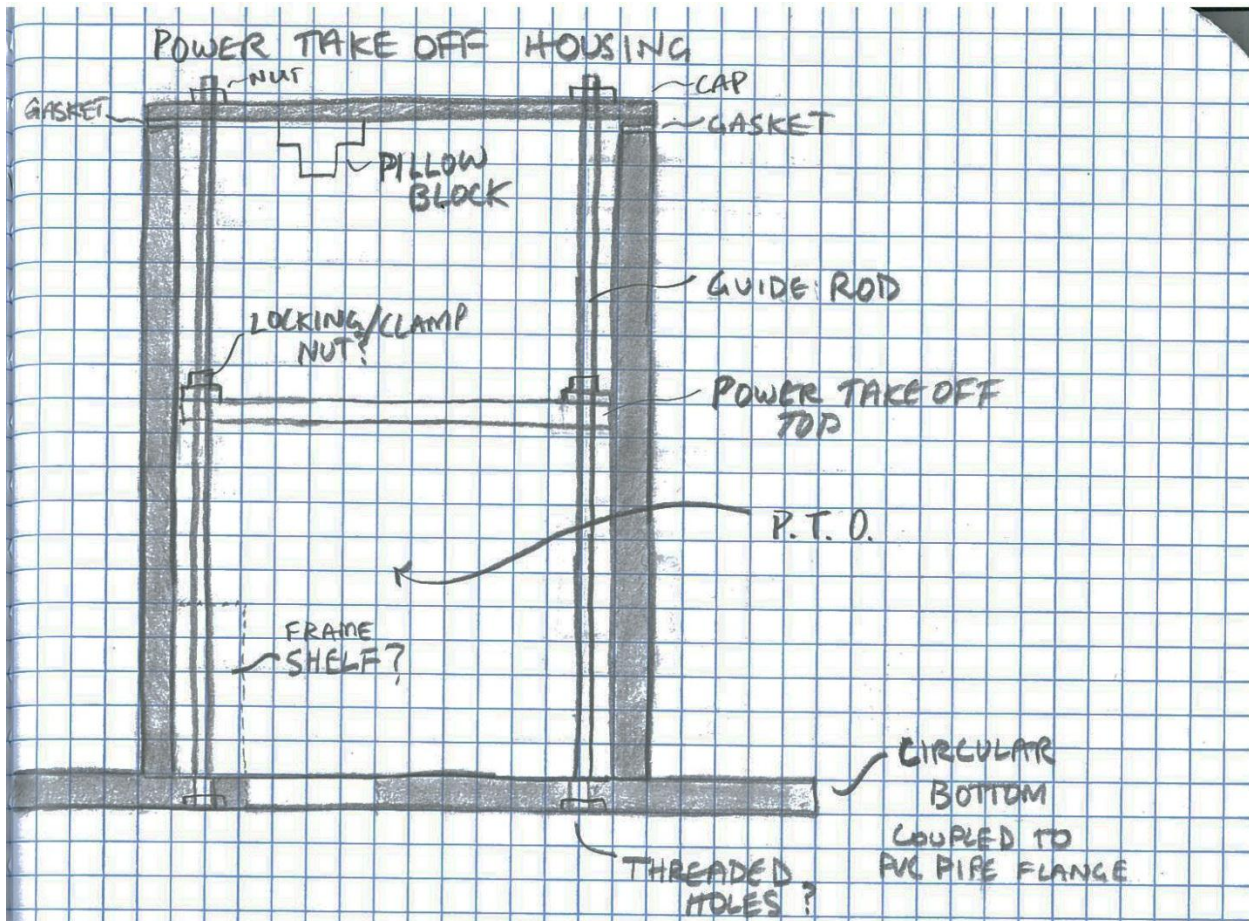
$$\frac{190}{204.79} = 0.9277 \text{ N}\cdot\text{m}$$

$$\frac{100}{204.79} = 0.4883 \text{ N}\cdot\text{m}$$

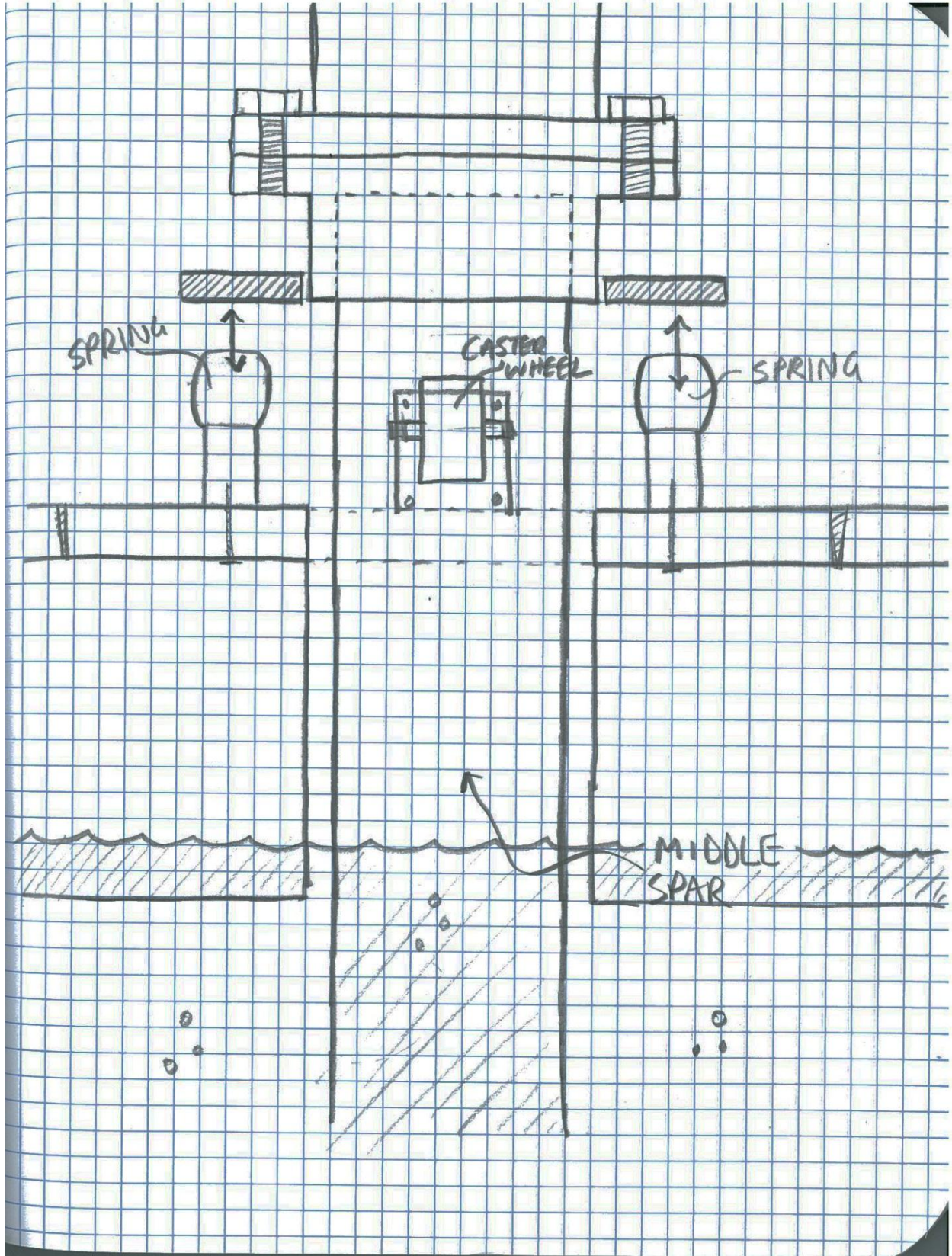


CURRENT SPAR BOTTOM CAP DESIGN





NOTE: SIDEWALLS/FLOOR/ROOF OF HOUSING  
 CONSTRUCTED W/ PLYWOOD (1/4 in) OR OTHER  
 SUITABLE WOOD, & SEALED W/ FIBERGLASS



## A.4 OPIE: Optical Positioning Instrumentation and Evaluation

To record the movement a buoy when it is in the water, the OPIE system is used to track points on the object being observed. This project created these points by drawing black dots that are approximately 3/8" in diameter the side of the buoy close to the water line. The OPIE system uses a camera to film the object of interest. In the wave tank OPIE can be mounted to view through a glass window on the side of the wave tank. The black dots on the side of the buoy are then defined in the program by choosing the points to track in a calibration picture by the user. The program moves through each frame, tracking the position of the black dots.



Figure 17: The OPIE camera pointed towards the window on the side of the wave tank.

The information gathered by the OPIE system is subsequently analyzed in Matlab. The OPIE Matlab code that accompanies the other OPIE software keeps data for heave, pitch, yaw, speed and other parameters. Output plots of the vertical displacement of the buoy with respect to time are used to determine the unknown system parameters.

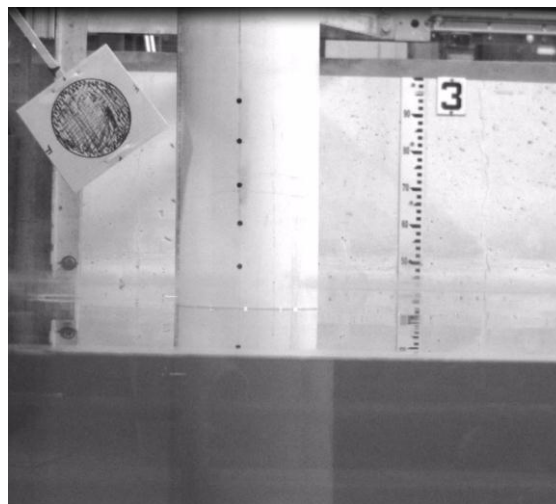
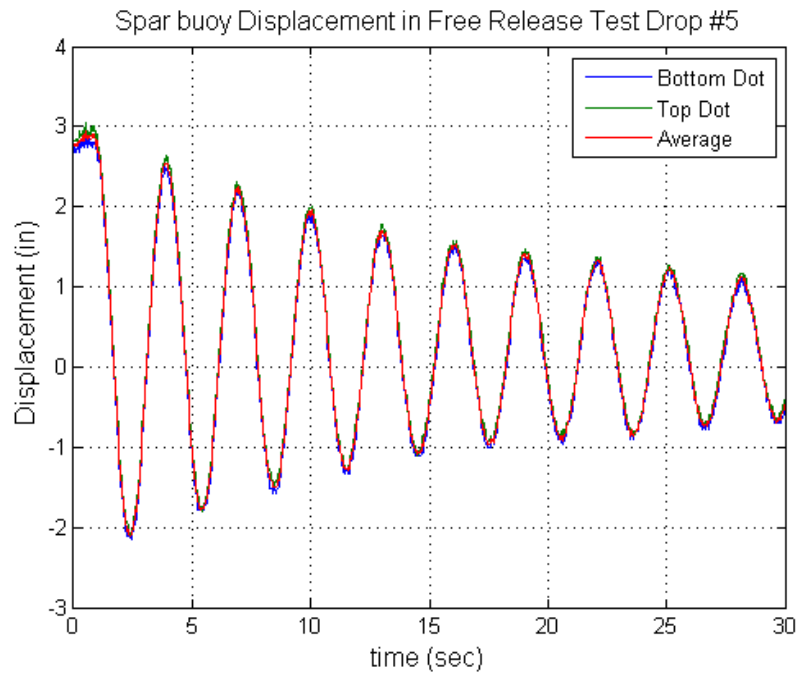
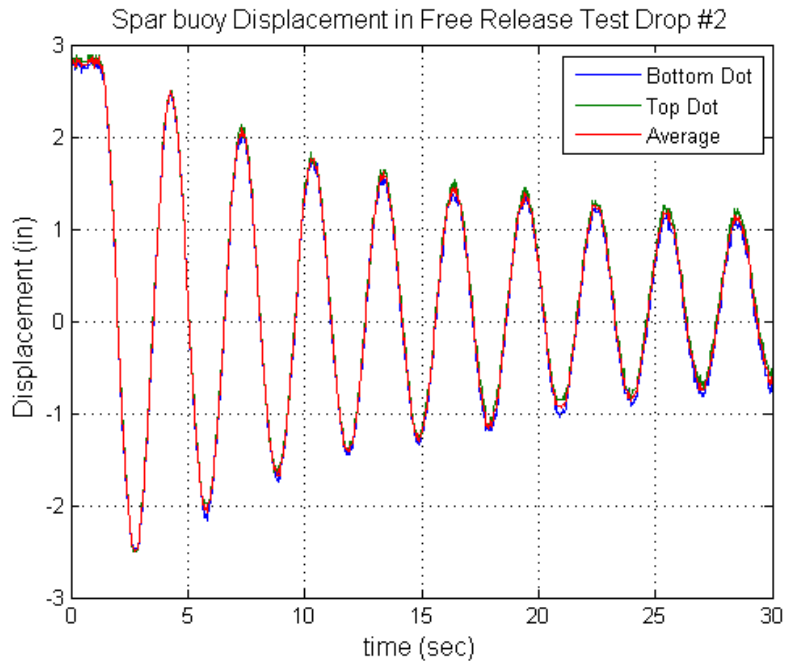
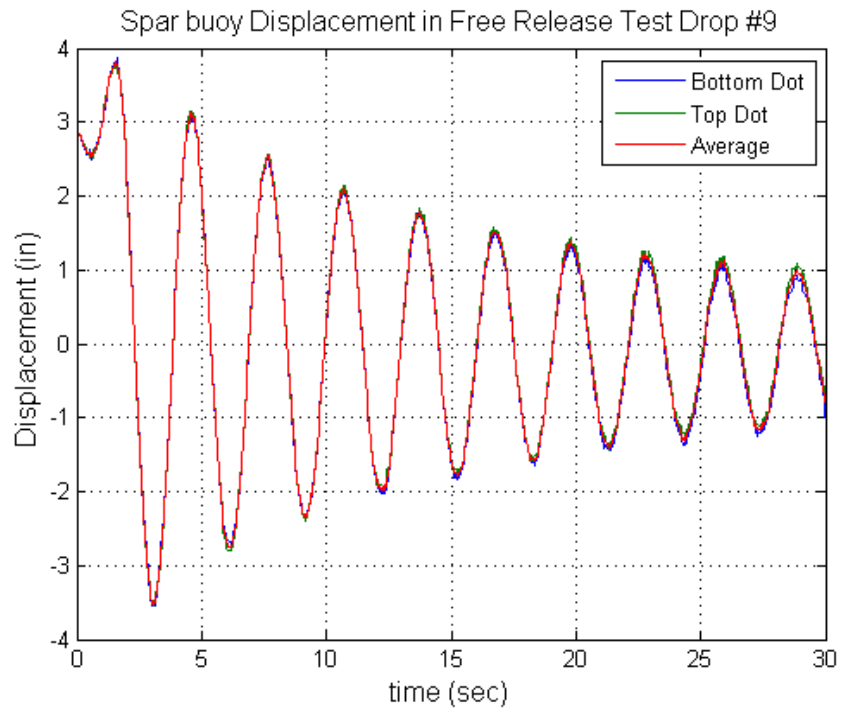


Figure 18: Frame grab of one of the videos recorded by the OPIE system during the spar free drop test. A series of black dots can be seen on the side of the spar. On the upper left side of the screen is a calibration circle of known dimensions. This circle is what OPIE bases all of its distance measurements off of.

## A.5 Additional Free Release Plots









## A.6 Bill of Materials and Final Budget as of 4/25/2014

<b>WECB BOM and Budget Calculations</b>		
Initial Budget:		\$2,950.00
<u>Item</u>	<u>Price</u>	<u>Budget Left</u>
2 clutch bearings	\$194.00	<b>\$2,756.00</b>
YAF Generator & Rectifier	\$393.38	<b>\$2,362.62</b>
8" PVC pipe	\$64.50	<b>\$2,298.12</b>
Pipe Cement	\$42.30	<b>\$2,255.82</b>
Flanges and Hardware	\$89.00	<b>\$2,166.82</b>
Gears	\$148.86	<b>\$2,017.96</b>
Bolts, Plexiglass	\$42.30	<b>\$1,975.66</b>
Aluminum stock (1/13)	\$52.44	<b>\$1,923.22</b>
Set Screws	\$16.06	<b>\$1,907.16</b>
Aluminum stock (1/22)	\$48.32	<b>\$1,858.84</b>
Steel and Al Stock (1/23)	\$80.69	<b>\$1,778.15</b>
Flex Coupling	\$22.04	<b>\$1,756.11</b>
Assorted Hardware (Bolts, Nuts, Wood, etc)	\$300.00	<b>\$1,456.11</b>
Large Threaded Rod (Tentative)	\$65.00	<b>\$1,391.11</b>
Fastenal Run 3/18	\$38.02	<b>\$1,353.09</b>
Marine Paint	\$15.81	<b>\$1,337.28</b>
Two Part Foam	\$54.00	<b>\$1,283.28</b>
Wheels	\$67.78	<b>\$1,215.50</b>
Ball Bearings and Delrin	\$85.25	<b>\$1,130.25</b>
Small Shaft Bearings	\$30.87	<b>\$1,099.38</b>
Second Miter Gear	\$24.91	<b>\$1,074.47</b>
Compression Springs	\$69.82	<b>\$1,004.65</b>
LEDs and Breadboards	\$216.89	<b>\$787.76</b>
Second Rectifier Circuit	\$16.99	<b>\$770.77</b>
Flex Coupling	\$72.37	<b>\$698.40</b>
Bolts, strapping	\$46.54	<b>\$651.86</b>
Marine Paint and Brushes	\$55.00	<b>\$596.86</b>
3.5' Diameter Surlyn Weather Buoy	Donated	
<b>TOTAL COST</b>		<b>\$2,353.14</b>